



# AMPK promotes survival of c-Myc-positive melanoma cells by suppressing oxidative stress

Alain Kfoury<sup>1,†</sup>, Marzia Armaro<sup>1,†</sup>, Caterina Collodet<sup>2,3</sup> , Jessica Sordet-Dessimoz<sup>1</sup>, Maria Pilar Giner<sup>2</sup>, Stefan Christen<sup>2</sup>, Sofia Moco<sup>2</sup>, Marion Leleu<sup>1</sup>, Laurence de Leval<sup>4</sup>, Ute Koch<sup>1</sup>, Andreas Trumpp<sup>5,6</sup>, Kei Sakamoto<sup>2,3</sup>, Friedrich Beermann<sup>1</sup> & Freddy Radtke<sup>1,\*</sup> 

## Abstract

Although c-Myc is essential for melanocyte development, its role in cutaneous melanoma, the most aggressive skin cancer, is only partly understood. Here we used the *Nras*<sup>Q61K</sup>*INK4a*<sup>-/-</sup> mouse melanoma model to show that c-Myc is essential for tumor initiation, maintenance, and metastasis. c-Myc-expressing melanoma cells were preferentially found at metastatic sites, correlated with increased tumor aggressiveness and high tumor initiation potential. Abrogation of c-Myc caused apoptosis in primary murine and human melanoma cells. Mechanistically, c-Myc-positive melanoma cells activated and became dependent on the metabolic energy sensor AMP-activated protein kinase (AMPK), a metabolic checkpoint kinase that plays an important role in energy and redox homeostasis under stress conditions. AMPK pathway inhibition caused apoptosis of c-Myc-expressing melanoma cells, while AMPK activation protected against cell death of c-Myc-depleted melanoma cells through suppression of oxidative stress. Furthermore, TCGA database analysis of early-stage human melanoma samples revealed an inverse correlation between C-MYC and patient survival, suggesting that C-MYC expression levels could serve as a prognostic marker for early-stage disease.

**Keywords** AMPK; c-Myc; gene targeting; melanoma; oxidative stress

**Subject Categories** Cancer

**DOI** 10.15252/emboj.201797673 | Received 26 June 2017 | Revised 12 January 2018 | Accepted 17 January 2018 | Published online 12 February 2018

**The EMBO Journal (2018) 37: e97673**

## Introduction

Malignant melanoma is an aggressive cancer of melanocytes and frequently originates in the skin. Cutaneous melanoma accounts for 80% of skin cancer-related deaths (Siegel *et al.*, 2013). Disease incidence and associated mortality rates increased continuously

over the years (Gray-Schopfer *et al.*, 2007; Purdie *et al.*, 2008). Neoplastic transformation of melanocytes results in mutations of proto-oncogenes, which often cause hyperactivation of the MAP-kinase pathway (Chin *et al.*, 2006). *BRAF*<sup>(V600E)</sup> and *NRAS*<sup>(Q61R)</sup> mutations are amongst the most frequent genetic aberrations found in patients with cutaneous melanoma. Mutation frequencies are 50–60% and 20%, respectively (Maldonado *et al.*, 2003; Curtin *et al.*, 2005; Xia *et al.*, 2014). Other genetic lesions, which predispose to human melanoma formation, are loss-of-function mutations of the *INK4A/ARF* locus (Chin, 2003). More recently, next-generation sequencing has been used to characterize the mutational landscape of human melanomas. These studies confirmed the presence of frequent driver mutations found in *BRAF* and *NRAS* but additionally identified novel genes whose mutations were associated with either *NRAS*- or *BRAF*-driven melanomas (Berger *et al.*, 2012; Xia *et al.*, 2014). Interestingly, approximately one-third of melanoma patients do not have any mutations in *NRAS* or *BRAF* indicating that other mutations, which do not necessarily lead to the hyperactivation of the MAP-kinase pathway, can also cause and/or influence progression of disease (Xia *et al.*, 2014).

The bHLH zipper Myc proto-oncogenic transcription factor family is comprised of three members: c-, L-, and N-Myc. Myc expression in adult tissues is generally low and restricted to stem or progenitor cells (Laurenti *et al.*, 2009). Myc function has been linked to many cellular processes including cell proliferation, growth, energy metabolism, and various biosynthetic pathways (Eilers & Eisenman, 2008; Kress *et al.*, 2015). Although *Myc* genes are not frequently mutated in tumors, they are recurrently overexpressed in a plethora of cancers. The reason being that Myc is a downstream effector of many signaling pathways that are involved themselves in oncogenic processes. Subsequently, Myc is upregulated during disease progression. Consistently, activating mutations in *MYC* genes have not been identified in human melanoma, but C-MYC has been found to be overexpressed in melanoma metastases as well as

1 Ecole Polytechnique Fédérale de Lausanne, School of Life Sciences, Swiss Institute for Experimental Cancer Research, Lausanne, Switzerland

2 Nestlé Institute of Health Sciences SA, Lausanne, Switzerland

3 Ecole Polytechnique Fédérale de Lausanne, School of Life Sciences, Lausanne, Switzerland

4 Institute of Pathology, University Hospital Lausanne, Lausanne, Switzerland

5 Division of Stem Cells and Cancer, Deutsches Krebsforschungszentrum (DKFZ), Heidelberg, Germany

6 Heidelberg Institute for Stem Cell Technology and Experimental Medicine (HI-STEM GmbH), Heidelberg, Germany

\*Corresponding author. Tel: +41 21 693 07 71; E-mail: freddy.radtke@epfl.ch

†These authors contributed equally to this work

in tumor-derived melanoma cell lines (Kraehn *et al*, 2001; Zhuang *et al*, 2008; Pouryazdanparast *et al*, 2012a). Overexpression of C-MYC in metastases has been linked to copy number gain (Gerami *et al*, 2011; Pouryazdanparast *et al*, 2012a). Functionally, c-Myc overexpression seems to be necessary to counteract oncogene-induced senescence in NRAS<sup>Q61R</sup>- or BRAF<sup>V600E</sup>-driven melanoma (Zhuang *et al*, 2008). Additional roles that c-Myc overexpression may play during metastasis of cutaneous melanoma are currently unknown.

While specific roles of c-Myc overexpression in melanoma require further analysis, the physiological function of Myc in melanocytes has been well established during development (Pshenichnaya *et al*, 2012). *c-Myc* loss of function (LoF) in melanocyte precursors resulted in reduced numbers of melanoblasts and mice revealed a hair graying phenotype. Interestingly, *c-Myc*-deficient melanocyte progenitors upregulated N-Myc. Combined LoF of *c-Myc* and *N-Myc* resulted in a complete loss of pigmentation indicating that (i) N-Myc partially compensates for loss of *c-Myc* and (ii) Myc is essential for the melanocytic lineage.

The present study employs a metastasizing *Nras*<sup>Q61K</sup>*INK4a*<sup>-/-</sup> mouse melanoma model (Ackermann *et al*, 2005; Pshenichnaya *et al*, 2012) to address the function of c-Myc and downstream target signaling for development, maintenance, and progression of disease. We assessed the functional role of c-Myc either by inactivating *c-Myc* or interfering with downstream target molecules. Results were compared and correlated to human melanoma for prognostic and predictive value of the disease.

## Results

### c-Myc is essential for initiation of Nras-driven INK4a-deficient melanoma

To investigate the role of c-Myc for melanoma development, we used a genetic LoF approach. We intercrossed mice carrying conditional alleles of *c-Myc* (*c-Myc*<sup>lox/lox</sup>; Trumpp *et al*, 2001) with transgenic melanoma-prone mice (*Tyr::Nras*<sup>Q61K</sup>*INK4a*<sup>-/-</sup>). The *Nras*<sup>Q61K</sup> oncogene is expressed under the control of the tyrosinase promoter in combination with loss of the tumor suppressor *INK4a* (Ackermann *et al*, 2005). In addition, tyrosinase-driven Cre-recombinase ensures efficient inactivation of conditional *c-Myc* alleles within the melanocytic lineage (*Tyr::Nras*<sup>Q61K</sup>*INK4a*<sup>-/-</sup>*c-Myc*<sup>lox/lox</sup> and *Tyr::Nras*<sup>Q61K</sup>*INK4a*<sup>-/-</sup>*c-Myc*<sup>lox/lox</sup>*Tyr::Cre* mice hereafter referred to as *Tyr::Nras*<sup>Q61K</sup>*INK4a*<sup>-/-</sup>*c-Myc*<sup>Δ/Δ</sup>) (Delmas *et al*, 2003; Ackermann *et al*, 2005; Pshenichnaya *et al*, 2012).

In agreement with previous reports (Ackermann *et al*, 2005), *Tyr::Nras*<sup>Q61K</sup>*INK4a*<sup>-/-</sup>*c-Myc*<sup>lox/lox</sup> mice developed primary naevi at age of 2 months that progressed with time to melanoma invading the reticular dermis and subcutis. At 6–7 months, 100% of the mice have developed melanoma and more than 30% showed metastases in lymph nodes (LN), lung, and other organs (Figs 1 and EV1A–L). In contrast, *Tyr::Nras*<sup>Q61K</sup>*INK4a*<sup>-/-</sup>*c-Myc*<sup>Δ/Δ</sup> mice did not develop melanoma within the investigated time frame, but a hair graying phenotype with normal skin morphology (Fig 1A and C). To test whether the incapacity of developing melanoma in *c-Myc*-mutant mice is simply a

consequence of melanocyte deficiency, we performed Fontana-Masson staining for melanin and also quantified cellular melanin content (Pshenichnaya *et al*, 2012) of the skin from *Tyr::Nras*<sup>Q61K</sup>*INK4a*<sup>-/-</sup>*c-Myc*<sup>lox/lox</sup>, *Tyr::Nras*<sup>Q61K</sup>*INK4a*<sup>-/-</sup>*c-Myc*<sup>Δ/Δ</sup>, C57BL/6, and NSG mice as controls. Positive staining confirmed the presence of residual melanocytes in the skin of *Tyr::Nras*<sup>Q61K</sup>*INK4a*<sup>-/-</sup>*c-Myc*<sup>Δ/Δ</sup> mice (Fig 1A). The melanin content of *Tyr::Nras*<sup>Q61K</sup>*INK4a*<sup>-/-</sup>*c-Myc*<sup>Δ/Δ</sup> mice was 15.9-fold reduced compared to *Tyr::Nras*<sup>Q61K</sup>*INK4a*<sup>-/-</sup>*c-Myc*<sup>lox/lox</sup> but comparable to C57BL/6 mice (Fig 1B). This is in agreement with a previous report showing that loss of c-Myc in the melanocytic lineage results in reduced although detectable numbers of melanocyte precursors causing a hair graying phenotype in *Tyr::Cre c-Myc*<sup>Δ/Δ</sup> mice (Pshenichnaya *et al*, 2012). The result indicates the inability to develop melanoma is not simply due to a complete loss of melanocytes during development.

### Increased c-Myc expression correlates with high tumor initiation potential and is preferentially confined to metastatic melanoma

We investigated next whether c-Myc protein expression may change during disease progression analyzing primary versus metastatic sites in our (*Tyr::Nras*<sup>Q61K</sup>*INK4a*<sup>-/-</sup>) melanoma animals. Thus, we made use of GFP-c-Myc knock-in reporter mice (*c-Myc*<sup>G/G</sup>), which express a functional GFP-c-Myc fusion protein (Huang *et al*, 2008). *c-Myc*<sup>G/G</sup> were intercrossed with *Tyr::Nras*<sup>Q61K</sup>*INK4a*<sup>-/-</sup> mice to generate *c-Myc*<sup>G/G</sup>*Tyr::Nras*<sup>Q61K</sup>*INK4a*<sup>-/-</sup> reporter animals (hereafter *c-Myc*<sup>rep</sup> mice) (Fig 2A). c-Myc protein expression in primary and metastatic tumors in *c-Myc*<sup>rep</sup> mice was analyzed at 7 months of age. Interestingly, CD45<sup>-</sup>CD31<sup>-</sup> melanoma cells revealed an increase in both relative numbers and expression levels of GFP-c-Myc-positive cells (hereafter c-Myc<sup>hi</sup>) at metastatic sites compared to primary tumor. At metastatic sites (LN, spleen, and lung), the percentage of c-Myc<sup>hi</sup> cells ranged from 36 to 85% compared to only approximately 4% at the primary tumor site (Fig 2B). Next, tumor initiation capacity was assessed comparing c-Myc<sup>hi</sup> melanoma cells versus c-Myc<sup>lo</sup> cells. Thus, one thousand CD45<sup>-</sup>CD31<sup>-</sup> c-Myc<sup>hi</sup> or <sup>lo</sup> cells were FACS sorted from primary tumors and transplanted in Matrigel™ subcutaneously (s.c.) into NSG mice. c-Myc<sup>hi</sup> cells initiated tumor growth within 25 days post-transplantation, while tumor growth of c-Myc<sup>lo</sup> cells was detectable only 90 days post-transplantation (Fig 2C). No metastases were observed. Ninety-five percent of tumor cells derived from c-Myc<sup>hi</sup> cells retained c-Myc expression at experimental end-stage analysis. Interestingly, 40% of melanoma cells derived from c-Myc<sup>lo</sup> cells were c-Myc<sup>hi</sup> 100 days post-transplantation indicating that c-Myc<sup>lo</sup> cells can give rise to c-Myc<sup>hi</sup> tumors (Fig 2C).

Previous reports identified the neural crest stem cell (SC) marker CD271 as a potential cancer SC marker in human melanoma (Boiko *et al*, 2010; Civenni *et al*, 2011). Whether CD271 could also be a potential cancer SC marker in our murine melanoma model, its expression was analyzed in *c-Myc*<sup>rep</sup> mice in primary and metastatic tumors. Although CD271 expression was mostly confined to c-Myc<sup>hi</sup> melanoma cells, transplantation experiments of CD271<sup>-</sup>c-Myc<sup>hi</sup>, CD271<sup>+</sup>c-Myc<sup>hi</sup> and CD271<sup>+</sup>c-Myc<sup>lo</sup>, CD271<sup>-</sup>c-Myc<sup>lo</sup> failed to confirm such cancer SC role for CD271 in our model. Differential CD271 expression of c-Myc<sup>hi</sup> cells did not significantly alter tumor initiation potential (Fig EV2).

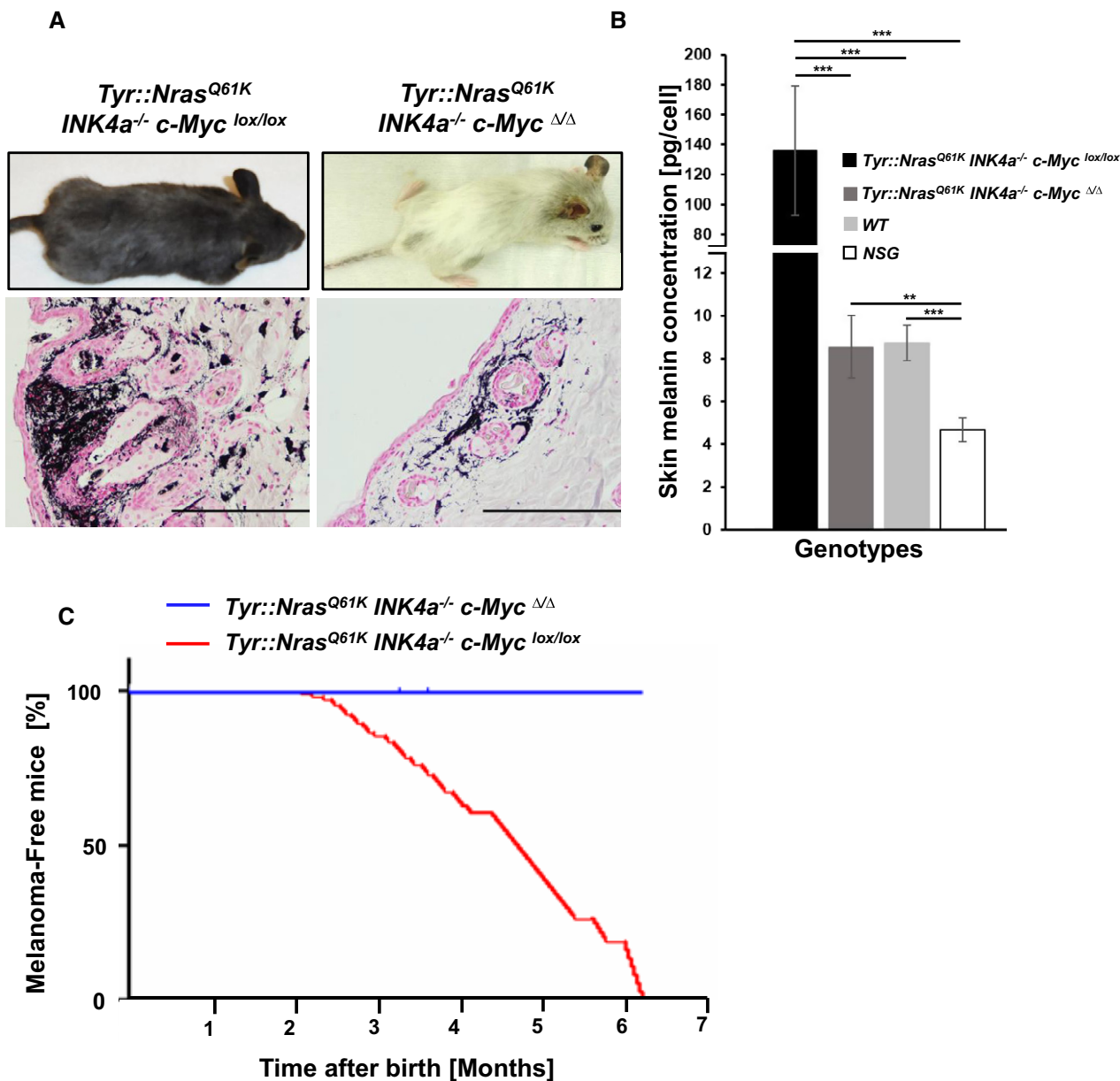


**Figure 1. c-Myc is essential for melanoma initiation in *Tyr::Nras<sup>Q61K</sup>INK4a<sup>-/-</sup>* mice.**

**A** Representative gross morphology of a *Tyr::Nras<sup>Q61K</sup>INK4a<sup>-/-</sup>c-Myc<sup>lox/lox</sup>* melanoma bearing mouse (4 months) and an age-matched tumor free *Tyr::Nras<sup>Q61K</sup>INK4a<sup>-/-</sup>c-Myc<sup>ΔΔ</sup>* mouse (top row). Histological analysis (Fontana-Masson stain) of skin sections derived either from a *Tyr::Nras<sup>Q61K</sup>INK4a<sup>-/-</sup>c-Myc<sup>lox/lox</sup>* mouse or from a *Tyr::Nras<sup>Q61K</sup>INK4a<sup>-/-</sup>c-Myc<sup>ΔΔ</sup>* mouse showing normal skin architecture (bottom row). Scale bars on images represent 200  $\mu$ m (40 $\times$  magnification).

**B** Bar graphs represent melanin concentration in the skin of indicated genotypes and are shown as mean  $\pm$  standard deviation (s.d.). A significant decrease (15.9-fold) in melanin concentration was observed in skin samples collected from *Tyr::Nras<sup>Q61K</sup>INK4a<sup>-/-</sup>c-Myc<sup>ΔΔ</sup>* animals ( $n = 7$ , dark gray bar) compared to *Tyr::Nras<sup>Q61K</sup>INK4a<sup>-/-</sup>c-Myc<sup>lox/lox</sup>* ( $n = 6$ , black bar). Skin samples from C57BL6/J ( $n = 5$ , light gray bar, WT) and NSG ( $n = 5$ , white bar) were included as base line and negative controls, respectively. Skin samples from 4-month-old animals were analyzed. Each sample was measured at least twice. \*\* $P < 0.03$ , \*\*\* $P < 0.01$ ; Student's  $t$ -test.

**C** Kaplan–Meier graph of melanoma incidence of *Tyr::Nras<sup>Q61K</sup>INK4a<sup>-/-</sup>c-Myc<sup>lox/lox</sup>* ( $n = 100$ ) and *Tyr::Nras<sup>Q61K</sup>INK4a<sup>-/-</sup>c-Myc<sup>ΔΔ</sup>* ( $n = 100$ ) mice, for melanoma incidence scoring refer to materials and methods.

Data information: See also Fig EV1.

### c-Myc is essential for survival of *Tyr::Nras<sup>Q61K</sup>INK4a<sup>-/-</sup>*-driven melanoma

Although c-Myc is essential for the initiation of *Tyr::Nras<sup>Q61K</sup>INK4a<sup>-/-</sup>*-driven melanoma and correlates with high tumor

initiation potential, its function in established melanoma is unclear. Thus, we generated two c-Myc-positive melanoma cell lines, mM1 and mM2, derived from *Tyr::Nras<sup>Q61K</sup>INK4a<sup>-/-</sup>* and *Tyr::Nras<sup>Q61K</sup>INK4a<sup>-/-</sup>c-Myc<sup>lox/lox</sup>* mice, respectively. We stably introduced a tamoxifen-inducible *Cre-ERT* transgene followed by

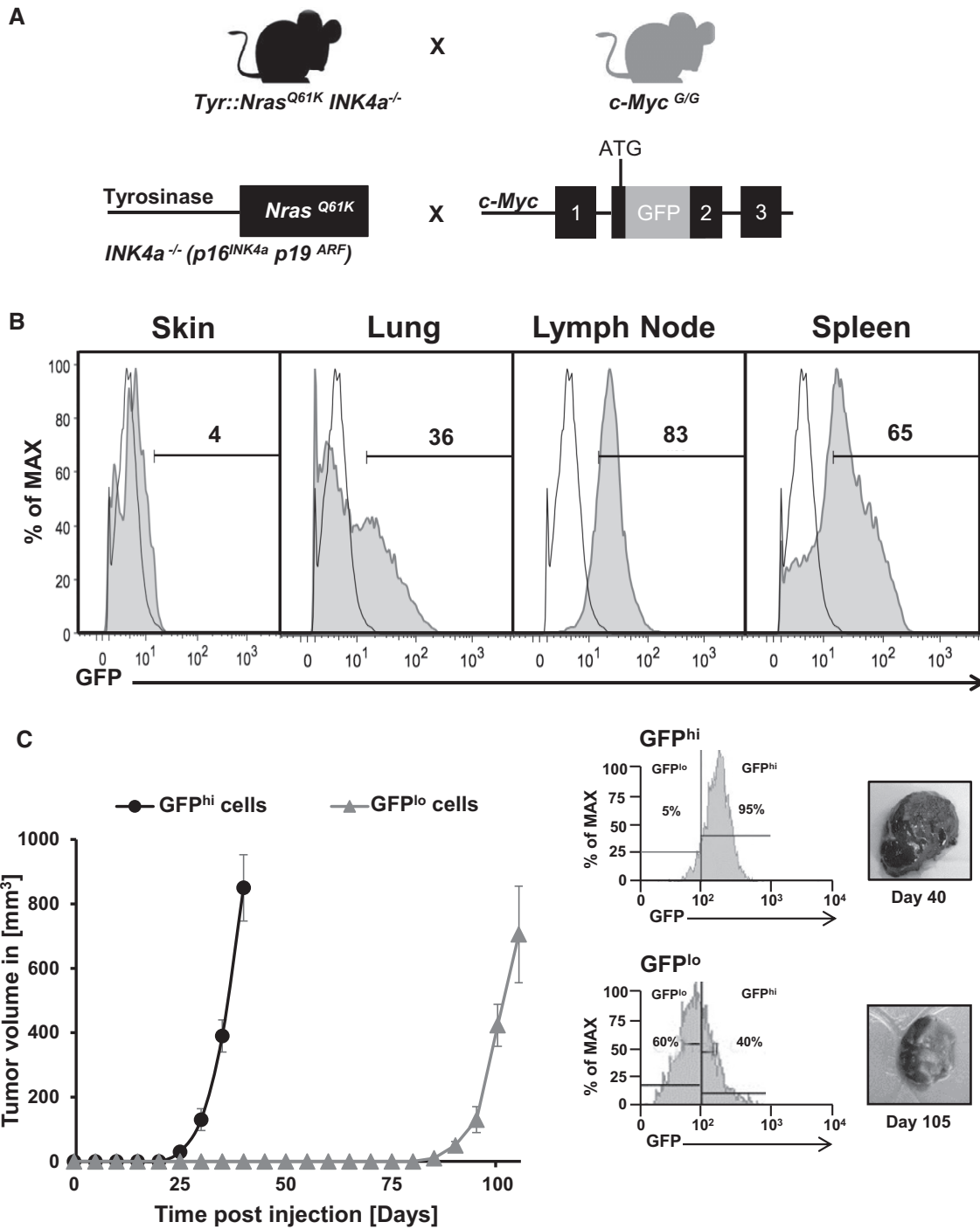


**Figure 2. c-Myc is preferentially expressed in metastatic melanoma and correlates with high tumor initiation potential.**

**A** Schematic depiction of the experimental strategy to generate a c-Myc reporter melanoma mouse model intercrossing *Tyr::Nras<sup>Q61K</sup>INK4a<sup>-/-</sup>* with *c-Myc<sup>G/G</sup>* reporter mice bearing a GFP cDNA targeted in frame into the second exon of the endogenous *c-Myc* locus generating *Tyr::Nras<sup>Q61K</sup>INK4a<sup>-/-</sup>c-myc<sup>G/G</sup>* animals.

**B** Histograms show representative flow cytometric analysis of GFP-c-Myc expression in melanoma cells (CD45<sup>-</sup>CD31<sup>-</sup>DAPI<sup>-</sup>) isolated from primary (skin) and metastatic sites (lymph node, lung, spleen) of 7-month-old *Tyr::Nras<sup>Q61K</sup>INK4a<sup>-/-</sup>c-myc<sup>G/G</sup>* mice (gray filled histograms). Numbers indicate percentage of GFP<sup>+</sup>c-Myc<sup>+</sup> cells. Melanoma cells from age-matched *Tyr::Nras<sup>Q61K</sup>INK4a<sup>-/-</sup>* mice (open histograms) were used as control (*n* = 3).

**C** Graph shows tumor initiation and growth of GFP-c-Myc (“hi”, black filled circles; GFP-c-Myc<sup>hi</sup>) and (“lo”, gray filled triangle; GFP-c-Myc<sup>lo</sup>) cells derived from metastatic lung melanoma of a *Tyr::Nras<sup>Q61K</sup>INK4a<sup>-/-</sup>c-myc<sup>G/G</sup>*, which were s.c. injected in Matrigel™ into NSG mice (*n* = 5 mice per group). Data points are presented as mean ± standard deviation (s.d.). Histograms show representative flow cytometric analysis of GFP-c-Myc expression after tumor resection at endpoint analysis as indicated (*n* = 3). GFP expression was analyzed on CD45<sup>-</sup>CD31<sup>-</sup>DAPI<sup>-</sup> cells. Pictures show gross morphology of s.c. grown tumors at endpoint analysis as indicated.

Data information: See also Fig EV2.

subsequent treatment with either vehicle (ETOH) or 4-OH-tamoxifen (4-OHT) to excise the conditional *c-Myc* alleles. Cell growth of mM2 *in vitro* was monitored using the alamarBlue® assay up to 72 h post-treatment. Vehicle-treated melanoma cells showed continuous cell growth (Fig 3A, left panel). In contrast, efficient *c-Myc*

inactivation as determined by Western blot analysis resulted in severely impaired growth and caused apoptosis of *Myc*-deficient cells (Fig 3B, left panel). Cre-ERT-infected melanoma mM1 cells grew normal in the presence of both ETOH and 4-OHT confirming that apoptosis is indeed a consequence of loss of *c-Myc* function

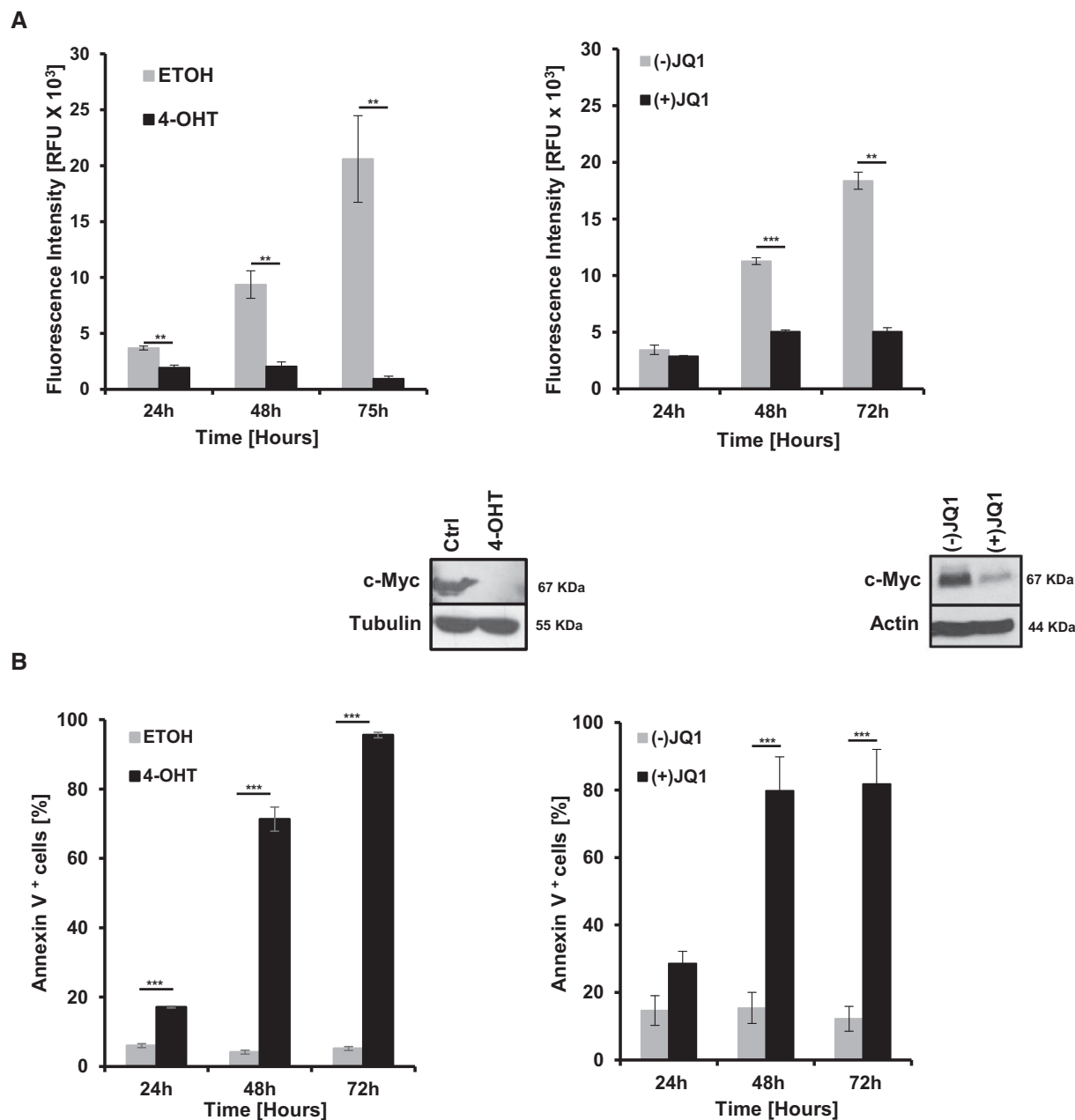


**Figure 3. c-Myc is essential for survival of *Tyr::Nras<sup>Q61K</sup>INK4a<sup>-/-</sup>*-driven melanoma *in vitro*.**

A, B Proliferation using the alamarBlue® staining assay (A) and analysis of apoptosis using AnnexinV/7AAD staining (B) was analyzed on *Tyr::Nras<sup>Q61K</sup>INK4a<sup>-/-</sup>c-Myc<sup>lox/lox</sup>* melanoma cells (mM2) stably expressing Cre-ERT. These cells were treated with either ethanol (ETOH) or 4-OH-tamoxifen (4-OHT) to inactivate the conditional *c-Myc* gene (left panels) or treated with the bromodomain inhibitor (+)JQ1 to lower *c-Myc* expression (right panels). The inactive (-)JQ1 enantiomer was used as vehicle control for (+)JQ1. Assays were performed at three independent time points (24, 48, and 72 h). Cre-ERT- or JQ1-mediated gene inactivation and expression of *c-Myc* was controlled by Western blot analysis 48 h after treatment. Data are presented as mean  $\pm$  standard deviation (s.d.) of one representative experiment. Two independent experiments were performed, and in each individual experiment, all data points were done in triplicates (\*\* $P < 0.03$ , \*\*\* $P < 0.01$ ; Student's *t*-test).

Data information: See also Fig EV3.



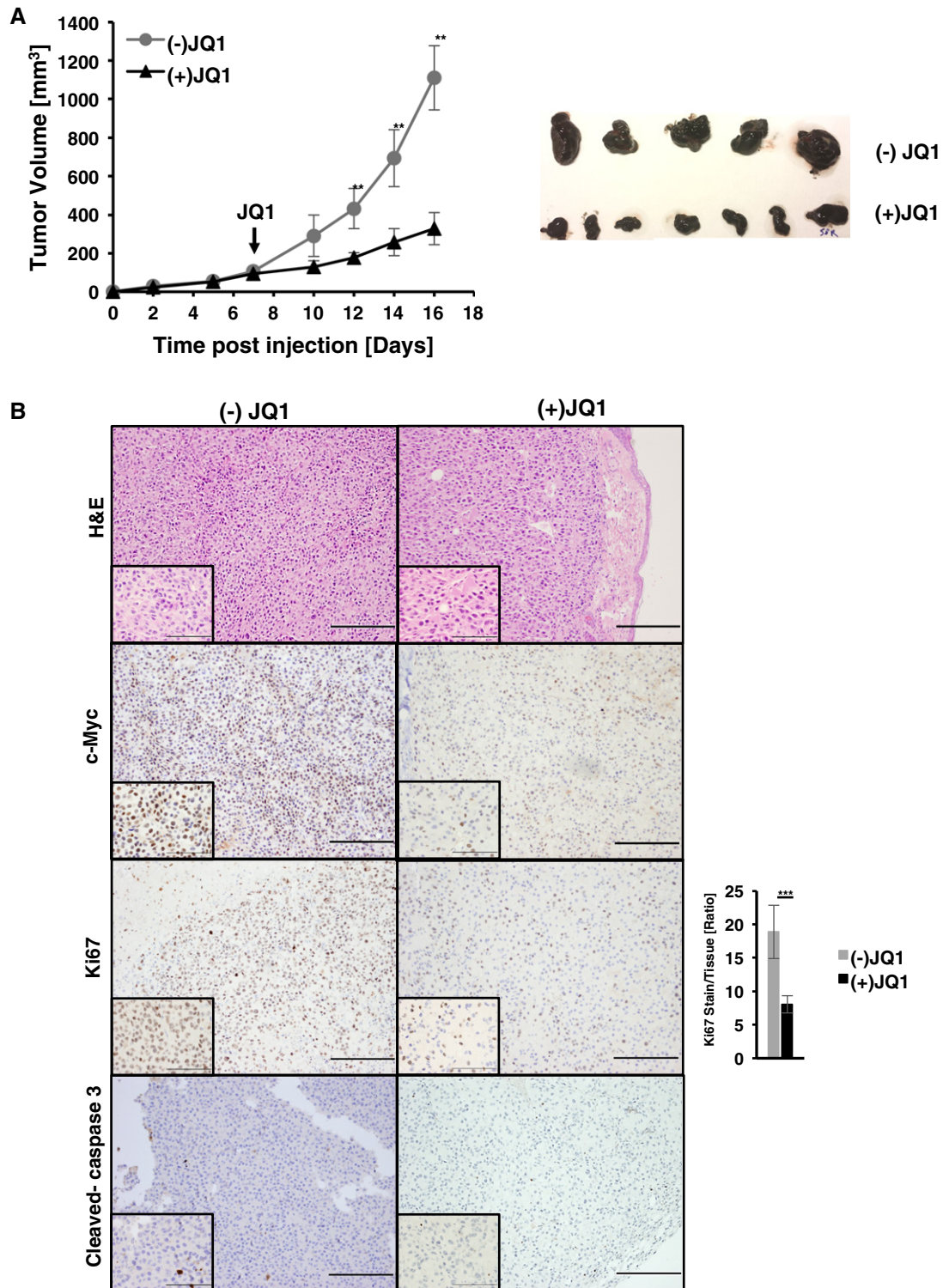


**Figure 4. c-Myc is essential for survival of *Tyr::Nras<sup>Q61K</sup>INK4a<sup>-/-</sup>*-driven melanoma *in vivo*.**

**A** Graph (left panel) shows tumor growth of *Tyr::Nras<sup>Q61K</sup>INK4a<sup>-/-</sup>c-Myc<sup>+/+</sup>* (mM1) melanoma cells injected s.c. ( $1 \times 10^5$  mM1 cells per mouse) in Matrigel™ into *Rag2 $\gamma$ <sup>-/-</sup>* mice. At day 7 post-transplantation, animals with a tumor volume of 100 mm<sup>3</sup> were randomized into two groups ( $n = 11$ /group), injected with either (-) JQ1 (gray filled circles; 50 mg/kg/day) or (+)JQ1 (black filled circles; 50 mg/kg/day) starting on day 7. For each time point, data are presented as mean  $\pm$  standard deviation (s.d.). At experimental endpoint, tumors were harvested for gross morphology (right panel) (\*\* $P < 0.03$ ; Student's *t*-test).

**B** Histological analysis of tumors excised 9 days post JQ treatment. Depicted are representative H&E, nuclear c-Myc, Ki67, and cleaved caspase-3 stainings on tumor sections taken from either (-) or (+)JQ-treated animals. Bar graph depicts quantification of Ki67-positive cells represented as mean  $\pm$  standard deviation (s.d.) ( $n = 5$  tumors for (-)JQ1 and 7 for (+)JQ1; \*\*\* $P < 0.01$ , Student's *t*-test). Scale bars on images represent 200  $\mu$ m and 100  $\mu$ m in insets.

and not due to 4-OHT treatment or aberrant Cre-ERT activity (Fig EV3A and B). Genetic *c-Myc* LoF results were further validated using the BET bromodomain protein inhibitor JQ1, which was previously shown to inhibit BRD4 at superenhancers, some of which are implicated in regulating *c-Myc* transcription (Delmore *et al*, 2011; Loven *et al*, 2013). BET inhibition by (+)JQ1 but not the (–)JQ1 enantiomer resulted in reduced *c-Myc* expression levels in mM1 and mM2 cells. This correlated with reduced cell growth and induction of apoptosis (Figs 3A and B, and EV3C). Reducing Myc protein levels in the frequently used B16F10 murine cell line revealed similar results (Fig EV3D).

To investigate *in vivo* whether tumor maintenance is *c-Myc* dependent,  $1 \times 10^5$  mM1 melanoma cells in Matrigel™ were injected s.c. into Rag2 $\gamma_c^{-/-}$  mice. Seven days post-transplantation, animals with a tumor volume of 100 mm<sup>3</sup> were randomized into two groups ( $n = 11$ /group) and treated either with (+) or (–)JQ1. Tumor growth of the (+)JQ1 treated cohort was significantly retarded compared to the (–)JQ1 group (Fig 4A). A similar experiment using another *Tyr::Nras<sup>Q61K</sup>INK4a<sup>-/-</sup>*-derived cell line (mM3) was performed to exclude the possibility that results are specific to mM1 cells (Fig EV3E). Furthermore, tumors were harvested at 5 and 9 days post JQ treatment for histological analysis of *c-Myc*, Ki67, and cleaved caspase-3 (Fig 4B). (+)JQ1-treated animals show reduced staining for *c-Myc* and Ki67, compared to tumors of the (–)JQ1-treated cohort. Quantification of Ki67-stained tumors indicates a reduction of 57% in (+) JQ1-treated tumors compared to (–)JQ1. Cleaved caspase-3 staining was comparable between the two cohorts indicating that *in vivo* (+) JQ1-mediated tumor growth retardation might mostly be due to inhibition of proliferation. Stainings were similar for both time points investigated. These results strongly suggest that *c-Myc* is essential for maintenance of transplanted melanoma cells *in vivo*.

### c-Myc alters gene expression of metabolic signaling pathways

We next wanted to elucidate potential mechanisms by which *c-Myc* exerts its essential function in *Nras/INK4a<sup>-/-</sup>*-driven melanoma. We sorted GFP-*c-Myc<sup>hi</sup>* and GFP-*c-Myc<sup>lo</sup>* cells from primary and metastatic tumor sites of *c-Myc<sup>rep</sup>* mice and performed gene expression analysis. In GFP-*c-Myc<sup>hi</sup>* compared to GFP-*c-Myc<sup>lo</sup>* melanoma cells, 13,993 genes were found to be significantly up- and 3,856 downregulated (Fig 5A). GO analysis indicated that metabolic processes followed by regulation of gene expression,

transcription, RNA biosynthesis, and cell-to-cell communication were amongst the most significantly changed processes in *c-Myc<sup>hi</sup>* melanoma cells (Fig 5B). Expectedly, many genes regulating RNA processing and transcription, cell cycle and growth, and migration and invasion were significantly upregulated in melanoma cells expressing *c-Myc* (Appendix Fig S1). KEGG pathway analysis pointed again to metabolic pathways including the 5'AMP-activated protein kinase (AMPK), mTOR, and PI3K–AKT pathways as the most significantly deregulated pathways (Fig 5C and D). We therefore focused on changes in metabolic gene signatures and tested the relevance of two important metabolic regulators 3-phosphoinositide-dependent protein kinase-1 (PDK1) and the AMPK signaling pathway. PDK1 is a master serine/threonine kinase important for the activation of AKT as well as other AGC kinases (Pearce *et al*, 2010) and was previously linked to melanoma (Scortegagna *et al*, 2014). Our reasoning to investigate the AMPK pathway closer was driven by the observation of increased expression of two isoforms of the  $\beta$  regulatory subunit of AMPK (*Prkab1* and *Prkab2*, which encode AMPK $\beta1$  and  $\beta2$ , respectively; Fig 5D) in *c-Myc*-positive melanoma cells. Additionally, AMPK is a central energy sensor, which plays critical roles in regulating metabolism and growth (Mihaylova & Shaw, 2011; Hardie *et al*, 2012). We knocked down *Pdpk1* (which encodes PDK1) and *Prkab2* in mM1 and mM2 cells. Knockdown of *Pdpk1* revealed a minor but significant effect on survival in mM2 melanoma cells. In contrast, knockdown of *Prkab2* induced apoptosis to a high percentage in both cell lines indicating that the AMPK pathway is functionally important for the survival of *c-Myc*-driven melanoma cells (Fig 5E). To further uncover a mechanistic function of *c-Myc* in melanoma, we focused more specifically on the AMPK signaling pathway.

### AMPK is important for survival of murine c-Myc-positive Tyr::Nras<sup>Q61K</sup>INK4a<sup>-/-</sup>-driven melanoma cells

AMP-activated protein kinase is a heterotrimer consisting of a catalytic subunit ( $\alpha$ ) and two regulatory subunits ( $\beta$  and  $\gamma$ ). In mammalian cells, there are two genes encoding the AMPK $\alpha$  catalytic subunit ( $\alpha1$ ,  $\alpha2$ ), two  $\beta$  genes ( $\beta1$ ,  $\beta2$ ), and three  $\gamma$  subunits ( $\gamma1$ ,  $\gamma2$ ,  $\gamma3$ ) (Hardie *et al*, 2012). As expression of some of these isoforms can be tissue specific (Bultot *et al*, 2016), we characterized the expression of the different AMPK isoforms in mM1 and mM2 cells

#### Figure 5. c-Myc expression in Tyr::Nras<sup>Q61K</sup>INK4a<sup>-/-</sup> melanoma cells alters gene expression profiles of metabolic signaling pathways.

- A Schematic depiction of the experimental design for RNA-seq analysis on isolated melanoma cells derived from *Tyr::Nras<sup>Q61K</sup>INK4a<sup>-/-</sup>c-myc<sup>CG</sup>* mice. Sorted GFP-*c-Myc<sup>hi</sup>* and GFP-*c-Myc<sup>lo</sup>* cells were gated on CD45<sup>+</sup>CD31<sup>+</sup>DAPI<sup>+</sup> cells, and RNA was isolated from GFP-*c-Myc<sup>hi</sup>* melanoma cells (two samples were derived from skin and one metastatic lymph node), and the GFP-*c-Myc<sup>lo</sup>* counterpart populations were used for RNA-seq (left panel). Right panel, pie chart indicates absolute and relative numbers of differentially expressed transcripts (upregulated transcripts in red and downregulated in blue) between GFP-*c-Myc<sup>hi</sup>* and GFP-*c-Myc<sup>lo</sup>* cells.
- B Gene ontology analysis on upregulated genes comparing GFP-*c-Myc<sup>hi</sup>* and GFP-*c-Myc<sup>lo</sup>* cells.
- C KEGG pathway analysis on upregulated genes comparing GFP-*c-Myc<sup>hi</sup>* and GFP-*c-Myc<sup>lo</sup>* cells.
- D Heatmap of RNA expression patterns comparing changes between GFP-*c-Myc<sup>hi</sup>* and GFP-*c-Myc<sup>lo</sup>* cells derived from skin (primary site) and LN (metastatic site) indicating major alterations of metabolic genes. Green indicates low and red high gene expression.
- E Quantification of apoptotic cells by AnnexinV/7AAD staining performed on two mouse melanoma cell lines mM1 and mM2 upon siRNA-mediated knockdown of *Pdpk1* (red bars) or *Prkab2* (green bars). Scrambled siRNA was used as control (siCtrl, blue bars). Data are presented as mean  $\pm$  s.d. of  $n = 3$  independent experiments. In each experiment, all samples were done in triplicates. Knockdown efficiencies of *Pdpk1* and *Prkab2* were controlled at the protein level by Western blot analysis (two right panels) 72 h post siRNA-mediated knockdown assessing AMPK $\beta2$  (siPrkab2) and PDK1 (siPdpk1) protein levels (\* $P < 0.05$ , \*\* $P < 0.03$ , \*\*\* $P < 0.01$ ; Student's *t*-test).

Data information: See Appendix Fig S1.

Source data are available online for this figure.

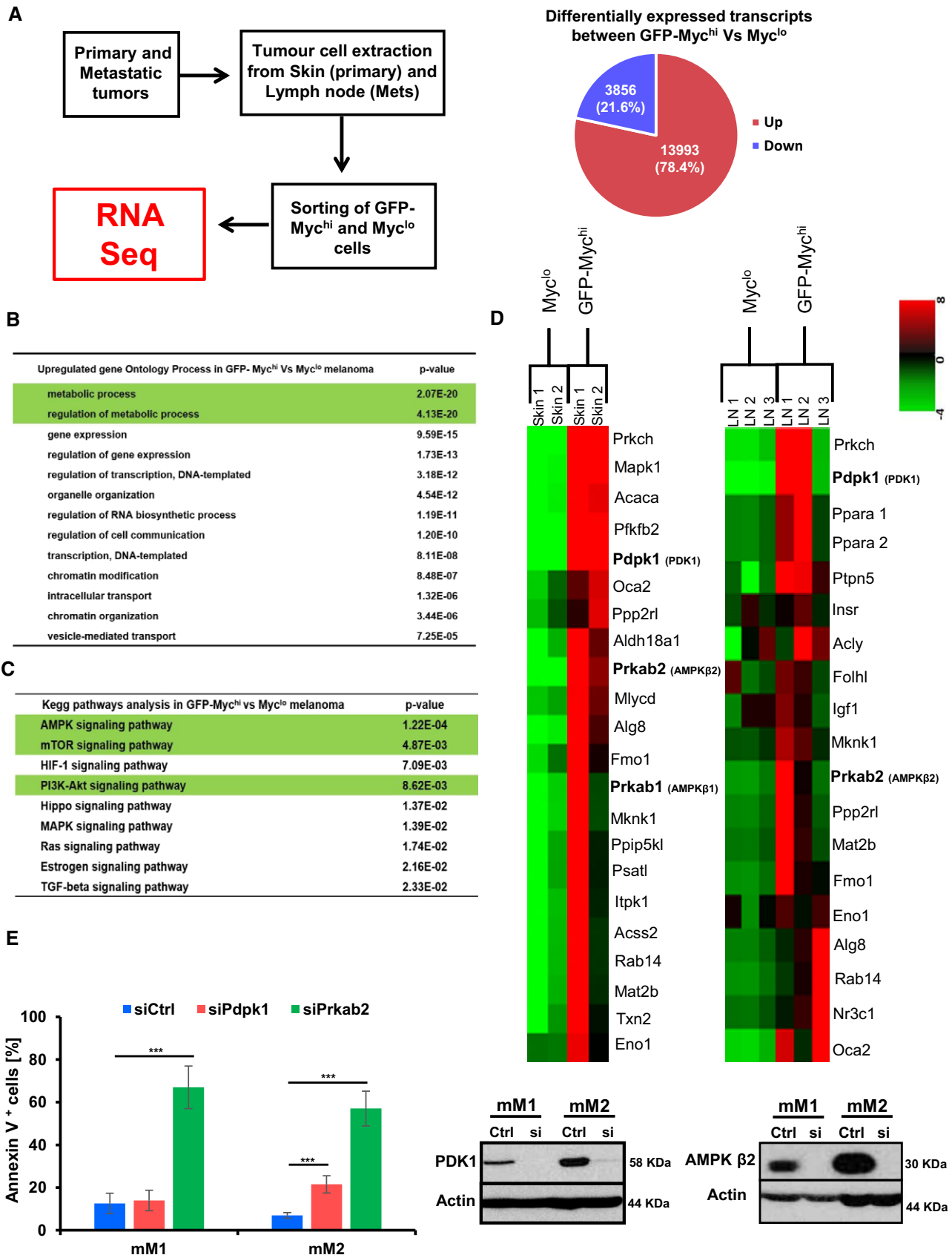


Figure 5.



with and without genetic inactivation or pharmacological inhibition of *c-Myc*. Protein extracts from mouse liver and skeletal muscle tissues were used as positive controls to account for different cell type-specific AMPK isoform expression. In mM1 and mM2 cells, AMPK $\alpha$ 1,  $\beta$ 1/ $\beta$ 2, and  $\gamma$ 1 are the predominantly expressed isoforms. Cre-ERT-mediated inactivation or pharmacological inhibition of *c-Myc* in mM2 and mM1 cells resulted in a pronounced reduction in AMPK $\alpha$ 1 and AMPK $\beta$ 2, while  $\beta$ 1 and  $\gamma$ 1 were unaffected (Fig 6A, left panels). To investigate whether reduced expression of AMPK $\alpha$ 1 and  $\beta$ 2 had affected downstream targets of AMPK, we monitored phosphorylation of various AMPK substrates in *c-Myc* sufficient versus *c-Myc*-depleted mM2 cells. mM2 *c-Myc*-depleted cells showed a robust reduction in phosphorylation of all tested AMPK substrates compared to control indicating that depletion of *c-Myc* protein results in reduced cellular AMPK activity (Fig 6A, right panel). Whether inhibition of AMPK is sufficient to cause cell death of *c-Myc*-positive melanoma cells, mM1 and mM2 cells were treated with either vehicle or the small molecule AMPK inhibitor dorsomorphin for 48 or 72 h, respectively. Dorsomorphin treatment resulted in AMPK inhibition as indicated by reduced pRaptor phosphorylation and correlated with increased numbers of apoptotic cells (Figs 6B and EV4A). Results for mM1 and mM2 cells were comparable. Although dorsomorphin is frequently used as an AMPK inhibitor, the same compound inhibits additional signaling pathways such as BMP or ALK (Vogt *et al*, 2011). To confirm that dorsomorphin-induced cell death of *c-Myc*-positive melanoma cells is indeed mediated through AMPK inhibition, we knocked down *Pkrab2* and *Prkaa1*, which encode for the AMPK $\beta$ 2 and  $\alpha$ 1 subunit in mM1, mM2, and B16F10 cells. Knockdown of *Pkrab2* as well as of *Prkaa1* resulted in increased cell death of *c-Myc*-positive melanoma cells (Figs 6C and D, and EV4B–D) confirming that AMPK is essential for survival of *c-Myc*-positive melanoma cells.

We then investigated whether AMPK activation would be sufficient to counteract at least partially the apoptotic phenotype in *c-Myc*-mutant melanoma cells. mM2 cells were treated with either vehicle or 4-OHT to activate Cre-ERT in the presence of DMSO or the highly specific allosteric AMPK activator, 991 (Xiao *et al*, 2013). The ability of 991 to activate AMPK was verified by analyzing phosphorylation of *bona fide* AMPK substrates by Western blot analysis

in MEFs and mM2 cells (Fig 6A and E right panel). As expected, lowering *c-Myc* levels genetically resulted in pronounced cell death of mM2 cells. In contrast, genetic depletion of *c-Myc* in the presence of 991 or the expression of a constitutive active form of AMPK $\alpha$ 1 (Crute *et al*, 1998) significantly prevented the induction of apoptosis in mM2 *c-Myc*-depleted cells (Figs 6E and EV4E). We further confirmed *in vivo* that (+)JQ1-treated melanoma bearing animals compared to (–)JQ1 treated animals revealed reduced p-AMPK staining in tumor sections (Fig EV4F). These results suggest that activation of the AMPK pathway downstream of *c-Myc* is important for survival of *c-Myc*-positive melanoma cells.

### AMPK suppresses ROS in *c-Myc*-positive melanoma cells

Unraveling mechanisms of cell death in *c-Myc*-depleted melanoma cells will elucidate how AMPK downstream of *c-Myc* ensures survival of tumor cells. Suppression of oxidative stress has been previously linked to the pro-tumorigenic properties of AMPK (Liu *et al*, 2012; Saito *et al*, 2015). We thus investigated whether *c-Myc*-depleted mM2 cells undergo apoptosis due to increased oxidative stress. We found that melanoma cells with reduced *c-Myc* significantly upregulated ROS (Fig 7A), which correlated with increased apoptosis (Fig 3B). To test whether increase in ROS is causative for induction of cell death, we treated *c-Myc*-depleted melanoma cells with the antioxidant/ROS scavenging agent  $\alpha$ -tocopherol.  $\alpha$ -tocopherol prevented ROS accumulation and rescued to a large extent *c-Myc*-depleted melanoma cells from cell death (Fig 7B). Since 991-driven AMPK activation significantly prevents apoptosis in *c-Myc*-depleted melanoma cells, we assessed whether this is mediated via suppression of oxidative stress. Activation of 991-mediated AMPK in *c-Myc*-depleted cells suppressed accumulation of ROS 48 h post-treatment (Fig 7C), which correlated with pronounced survival compared to vehicle-treated cells (Fig 6E). Therefore, depletion of *c-Myc* and subsequent downregulation of AMPK signaling compromise survival partially by inducing oxidative stress-mediated cell death. It appears that AMPK functions to counterbalance for deregulated *c-Myc*-induced biosynthesis, and if so, the need for AMPK could be alleviated by attenuating *c-Myc*-induced biosynthesis. Thus, mM1 and mM2 cells were treated with the AMPK inhibitor

**Figure 6. *c-Myc* ensures survival of *Tyr::Nras<sup>Q61K</sup>INK4a<sup>-/-</sup>* melanoma cells via AMPK pathway.**

- A Protein expression profiling of the different AMPK isoforms in mM2 mouse melanoma cells in steady state and upon *c-Myc* inactivation assessed by Western blot analysis 48 h after indicated treatments. Protein extracts from mouse liver and skeletal muscle tissues were used as positive controls for different AMPK isoforms (left and middle panel). Right panel shows phosphorylation status of known AMPK targets in the mM2 mouse melanoma cell line in steady state and upon *c-Myc* inactivation.
- B Quantification of apoptotic cells using AnnexinV/7AAD staining of mM2 melanoma cells 48 or 72 h after treatment with either the AMPK inhibitor dorsomorphin (black bars) or vehicle control (light gray bars). Data are presented as mean  $\pm$  s.d. of one representative out of two independent experiments. In each experiment, all samples were done in triplicates. Dorsomorphin inhibition efficiency on the AMPK pathway was monitored by Western blot analysis assessing phosphorylation of Raptor (pS792Raptor).
- C, D Quantification of apoptotic cells using AnnexinV/7AAD staining of mM2 melanoma cells 48 or 72 h post siRNA-mediated knockdown of AMPK $\beta$ 2 or AMPK $\alpha$ 1 (black bars) versus control siRNA (light gray bars). Data are presented as mean  $\pm$  s.d. of one representative out of three independent experiments. In each experiment, all samples were done in triplicates. Knockdown efficiency of AMPK $\beta$ 2 or AMPK $\alpha$ 1 was confirmed by Western blot analysis at 48 and 72 h post-treatment.
- E Quantification of apoptotic cells by AnnexinV/7AAD staining of mM2 melanoma cells 24 and 48 h post Cre-ERT-mediated inactivation of *c-Myc* in presence or absence of the AMPK activator 991. Ethanol (ETOH) and DMSO were used as vehicle controls. Data are presented as mean  $\pm$  s.d. of one representative out of two independent experiments. In each experiment, all samples were done in triplicates. Knockdown efficiency of *c-Myc* was confirmed by Western blot analysis 48 h after treatment.

Data information: \*\* $P < 0.03$ , \*\*\* $P < 0.01$ ; Student's *t*-test.

Source data are available online for this figure.

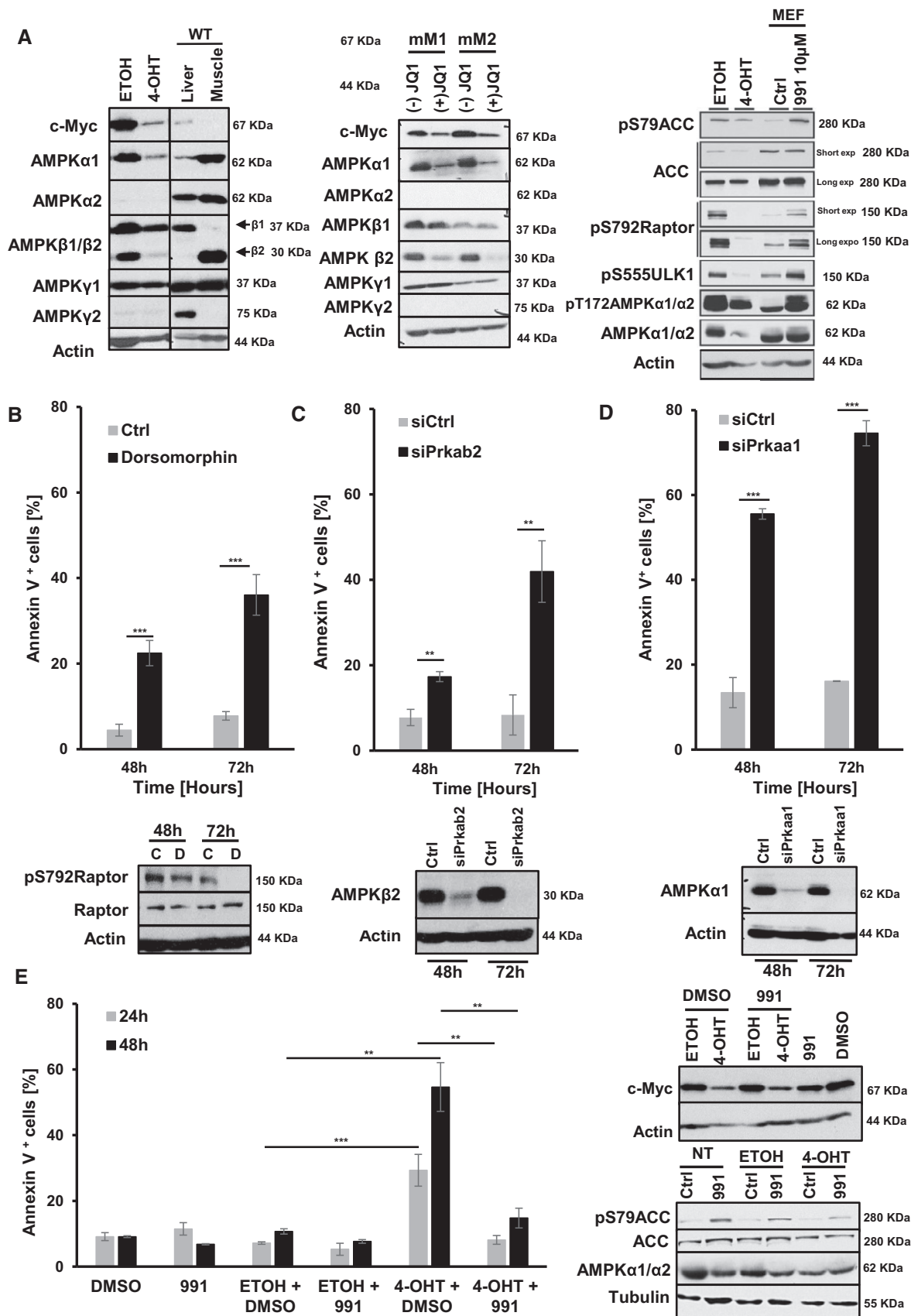


Figure 6.

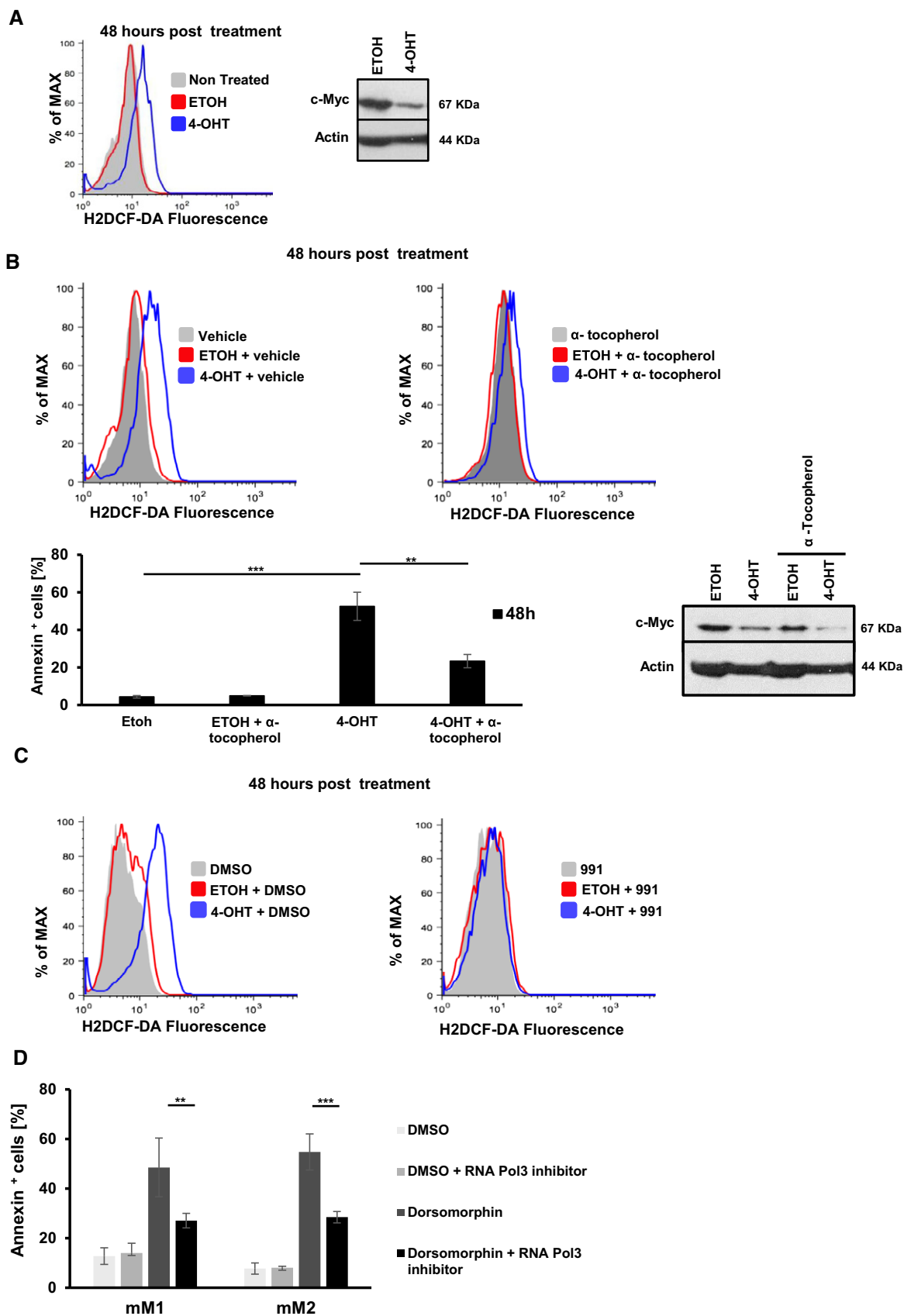


Figure 7.

**Figure 7. AMPK suppresses ROS in c-Myc-positive *Tyr::NRAS<sup>Q61K</sup>/INK4a<sup>-/-</sup>* melanoma cells.**

- A Representative flow cytometric histograms showing ROS production measured by the H2DCF-DA probe in mM2 cells 48 h post c-Myc inactivation (blue line, 4-OHT). Ethanol (red line, ETOH) was used as vehicle control. Gray filled histograms represent untreated cells ( $n = 3$ ). Deletion of c-Myc was assessed by Western blot analysis.
- B Representative flow cytometric histograms (top panels) showing ROS production measured by the H2DCF-DA probe in mM2 cells 48 h post c-Myc inactivation (blue line, 4-OHT) in the absence (vehicle; left panel) or presence (right panel) of the antioxidant vitamin E ( $\alpha$ -tocopherol, 100  $\mu$ M). Ethanol (red line, ETOH) was used as vehicle control. Gray filled histograms represent vehicle alone or  $\alpha$ -tocopherol alone treated cells. Bar diagram represents quantification of apoptotic cells by AnnexinV/7AAD staining of mM2 melanoma cells 48 h post-inactivation of c-Myc in the presence or absence of the antioxidant vitamin E ( $\alpha$ -tocopherol, 100  $\mu$ M). Ethanol (ETOH) or 4-OH-tamoxifen (4-OHT) was used as vehicle control (left bottom panel). Deletion efficiency of c-Myc was controlled by Western blot analysis (right bottom panel).  $^{**}P < 0.03$ ,  $^{***}P < 0.01$ , Student's  $t$ -test.
- C Representative flow cytometric histograms showing ROS production measured by the H2DCF-DA probe in mM2 cells 48 h post c-Myc inactivation in the presence or absence of the AMPK activator 991. Ethanol (ETOH) and DMSO were used as vehicle controls. Two independent experiments were performed.
- D Bar graph depicts quantification of apoptotic cells using AnnexinV/7AAD staining of mM1 and mM2 melanoma cells 48 h post-treatment: DMSO (white bar), DMSO + RNA Pol III inhibitor (light gray bar, 50  $\mu$ M), dorsomorphin (dark gray bar, 10  $\mu$ M), and RNA Pol III inhibitor + dorsomorphin (black bar, 50  $\mu$ M and 10  $\mu$ M, respectively).

Data information: Data are presented as mean  $\pm$  s.d. of one representative out of three independent experiments. In each experiment, all samples were done in triplicates.  $^{**}P < 0.03$ ,  $^{***}P < 0.01$ , Student's  $t$ -test. Source data are available online for this figure.

dorsomorphin in presence or absence of a RNA Pol III inhibitor, which slows down c-Myc-induced t-RNA and ribosome biogenesis. Dorsomorphin-induced apoptosis was significantly reduced in both mM1 and mM2 cells treated with the Pol III inhibitor (Fig 7D) supporting the hypothesis that AMPK provides a negative feedback loop for Myc-induced biosynthesis. Moreover, we monitored cellular energy status by measuring adenine nucleotide levels (ATP, ADP, and AMP) in control and Myc-depleted mM2 cells using ultra-high performance liquid chromatography mass spectrometry (Pluskal *et al*, 2010; Fig EV5). Genetic c-Myc depletion caused a robust and significant decrease in ATP and ADP levels, while AMP levels were not significantly altered, indicating that c-Myc is an important driving force for ATP production. Consistent with the results of c-Myc depletion, knockdown of AMPK $\alpha$ 1/2 resulted also in significantly decreased ATP and ADP levels (Fig EV5). The reduction in ATP and ADP levels in AMPK knockdown cells was less pronounced compared to c-Myc-depleted cells, which is consistent with the possibility that c-Myc exerts its important function in ATP biosynthesis not exclusively through AMPK.

**Elevated C-MYC expression correlates with reduced median survival of melanoma patients**

Our data indicate that elevated c-Myc protein expression is preferentially confined to metastatic sites in our mouse melanoma model. To investigate whether this is also the case in human melanoma, we tested C-MYC protein expression in 15 patient-derived human

melanoma cell lines (Caballero *et al*, 2010; Nikolaev *et al*, 2011). They were either derived from primary tumors (5 cell lines) or from metastatic sites (10 cell lines). Three out of five melanoma cell lines from the primary tumor site showed low but detectable protein C-MYC expression (LAU-T126, LAU-T921A, and LAU-Me36), whereas in the two remaining cell lines (LAU-Me300 and LAU-Me 300A) C-MYC expression was below detection limit. In contrast, 7 (LAU-Me 252, LAU-Me275, LAU-T618A, LAU-T1194, LAU-T12, LAU-T38713, and LAU-T33) out of 10 melanoma cell lines derived from metastatic melanoma patient samples showed high C-MYC expression levels (Fig 8A). There was no correlation between C-MYC expression levels and NRAS or BRAF-mutated patient samples, as C-MYC expression was detected in either patient samples. To investigate the MYC-AMPK-ROS connection in human melanoma samples, we first analyzed the protein composition of the AMPK subunits in tumor cell lines of primary (LAU-T921A) and metastatic (LAU-Me 252) origin with low C-MYC expression and two of metastatic origin (LAU-Me275, LAU-T333A) with high C-MYC expression. All AMPK subunits were expressed though at different levels in the cell lines investigated, with the exception of AMPK $\alpha$ 2 in LAU-T333, which was not detected (Fig 8B). To test whether AMPK signaling in these four cell lines is important for survival, we knocked down PRKAA1/2 (AMPK $\alpha$ 1/2). Interestingly, knockdown of AMPK $\alpha$ 1/2 induced apoptosis and ROS production significantly in LAU-T921A and LAU-Me252 cells with high C-MYC levels, while survival and ROS production was not significantly changed in LAU-T921A- and LAU-Me 252-expressing low levels of C-MYC (Fig 8C and D).

**Figure 8. Elevated C-MYC expression in human metastatic cell lines.**

- A Protein expression of C-MYC in 15 human melanoma cell lines (5 primary = 1° skin tumors and 15 from metastatic origin) was assessed by Western blot analysis. Protein extracts from human melanocytes were included as negative control.
- B Protein expression profiling of human AMPK isoforms in melanoma cell lines (one primary and three metastatic) was performed by Western blot analysis.
- C Quantification of apoptotic cells using AnnexinV/7AAD staining of human melanoma lines 48 h post siRNA-mediated knockdown of AMPK $\alpha$ 1 (black bars) or control siRNA (light gray bars). Data are presented as mean  $\pm$  s.d. of one representative out of two independent experiments. In each experiment, all samples were done in triplicates ( $^{***}P < 0.01$ ; Student's  $t$ -test). Knockdown efficiency of AMPK $\alpha$ 1 was confirmed by Western blot analysis 48 h post-treatment.
- D Representative flow cytometric histograms showing ROS production measured by the H2DCF-DA probe in human melanoma cell lines (one primary and three metastatic) 48 h post siRNA-mediated knockdown of AMPK $\alpha$ 1 (solid blue line) or control siRNA (solid red line). Three independent experiments with comparable results were performed.

Source data are available online for this figure.

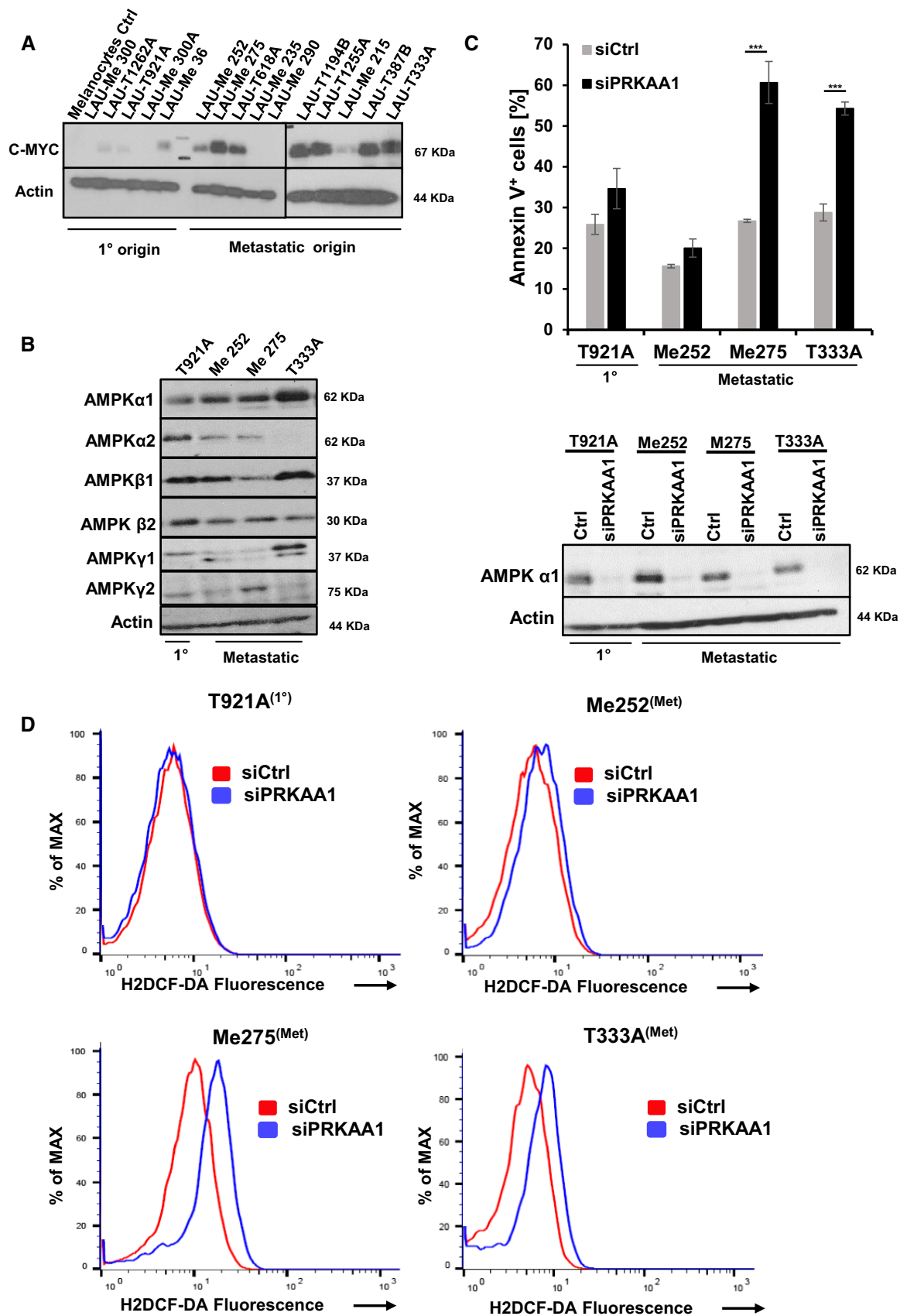


Figure 8.



Next, we performed immunohistochemical analysis for C-MYC and p-AMPK on paraffin sections of unpaired patient-derived tissue samples (eight patients—four primary tumors stage III-IV and four metastatic tumors). No C-MYC or p-AMPK expression was detected in the four primary tumors, whereas all samples from metastatic sites (axillary region or liver) stained positive for C-MYC and p-AMPK (Fig 9A). We further analyzed paired tumor samples from 10 patients by immunostaining for C-MYC and p-AMPK to obtain a better understanding of C-MYC and p-AMPK expression during melanoma progression. In five cases (patients 2 and 7–10), C-MYC expression was enhanced in metastatic compared to primary tumors, whereas in four patient samples (3–6) C-MYC immunostaining was comparable between primary tumors and metastasis (Fig 9B). Furthermore, five out of six patients (5, 6, 8–10) with low C-MYC expression in the primary tumor were also low for p-AMPK expression. Moderate to high p-AMPK staining was found in 5 out of 10 metastatic patient samples (2, 4, 6, 7, and 10) three of which correlated with high C-MYC expression (patients 4, 7, and 10) indicating that high p-AMPK-expressing patients represent a subgroup of the high C-MYC-expressing population. Interestingly, patients whose primary tumor samples were weakly to moderately positive (below 50%) for C-MYC had a longer time interval until occurrence of metastasis compared to patients in which the primary tumor sample had already high (over 50%) to very high (all cells) C-MYC levels (Fig 9B).

To test whether C-MYC expression levels might correlate with poor prognosis, we analyzed TCGA database case sets and correlated survival of melanoma patients based on C-MYC RNA expression of 352 patients, which were classified into high- and low-expressing cohorts. The high expression cohort corresponds to the 33% ( $n = 110$ ) of patients expressing highest C-MYC RNA levels, whereas the low cohort includes the 33% ( $n = 111$ ) of patients with the lowest expression. The Kaplan–Meier plot demonstrates that the patient cohort with high C-MYC RNA expression levels has a significant reduction in median survival time (MST) of 3.6 years compared to patients with low C-MYC expression (Fig 9C). The difference is even more significant if analysis of melanoma patients is based on C-MYC protein expression correlated with tumor T stage at diagnosis. The analysis was performed on a cohort of 197 patients for which C-MYC protein expression levels and corresponding tumor pathology information were available. Melanoma patients were divided into four groups: C-MYC<sup>lo</sup>/T0-2; C-MYC<sup>hi</sup>/T0-2; C-MYC<sup>lo</sup>/T4b; and C-MYC<sup>hi</sup>/T4b. Differential C-MYC protein expression did not correlate with MST in T4b patients. In contrast, high

C-MYC protein expression in T0-2 patients correlated significantly with reduced MST. The difference in reduced MST between the C-MYC high and low patient cohorts was > 4.9 years (Fig 9D). These data support the hypothesis that elevated C-MYC expression at early-stage melanoma correlates well with reduced patient MST. Whether AMPK expression levels might correlate with poor prognosis, TCGA database case sets were analyzed and correlated with survival of melanoma patients based on AMPK $\alpha$  protein expression of 192 patients. They were classified into the 33<sup>rd</sup> percentile of patients with highest and lowest expression. Although not significant, patients that survive beyond 3 years of diagnosis show a clear trend with reduced MST of 5.8 years between AMPK $\alpha$  high and low patient cohorts (Fig 9E).

## Discussion

c-Myc is one of the best-studied oncogenes promoting tumorigenesis in many tissues (Kress *et al*, 2015; Dejure & Eilers, 2017; Kalkat *et al*, 2017). It is frequently over expressed in cancer, correlates with tumor aggressiveness and poor clinical outcome (Nesbit *et al*, 1999; Beroukhim *et al*, 2010). Although gene-targeting experiments for c-Myc have revealed an essential role during melanocyte development (Pshenichnaya *et al*, 2012), its function in cutaneous malignant melanoma is not well known. Here, we have used a tyrosinase *Nras*<sup>Q61K</sup>-driven *INK4a*-mutant melanoma mouse model (Ackermann *et al*, 2005) to demonstrate that c-Myc is essential during initiation, progression, and maintenance of disease, in part through activating AMPK signaling to suppress oxidative stress.

Ablation of c-Myc during tumor initiation never led to melanoma formation, but instead, similar to wild-type mice with melanocyte-specific c-Myc inactivation, exhibited a hair graying phenotype. The hair graying phenotype is the consequence of reduced numbers of melanoblasts, which still developed into functional melanocytes (Pshenichnaya *et al*, 2012). Interestingly and in agreement with this study, residual melanocytes were also detected in our c-Myc-mutant melanoma mouse model suggesting that the inability to develop melanoma is not simply a consequence of lack of melanocytes. Why remaining melanocytes do not develop into melanoma is currently unknown. However, it is possible that c-Myc is essential for proliferation and thereby for the expansion of tumor-initiating cells. The fact that none of the c-Myc-mutant melanoma mice developed disease strongly suggests

**Figure 9. High C-MYC expression in melanoma patients correlates with reduced median survival.**

- C-MYC (set of two left panels) as well as p-AMPK (set of two right panels) immunostaining was performed on sections from primary (skin; top row) and metastatic (axillary region, middle row; liver, bottom row) of melanoma patient biopsies. A 5 $\times$  gross morphology panel set and a 40 $\times$  high magnification are depicted. Scale bars represent 2.5  $\mu$ m (5 $\times$ ) and 100  $\mu$ m (40 $\times$ ).
- Table shows semi-quantitative evaluation of C-MYC and p-AMPK expression in primary and metastatic melanomas of 10 paired biopsies (skin, Clark/Breslow stages III and IV) and the time interval between the examined samples. Grading is indicated in the footnote.
- Kaplan–Meier survival graph plots C-MYC RNA expression levels of 221 melanoma patients derived from TCGA database, divided into two groups C-MYC<sup>lo</sup> (blue line) versus C-MYC<sup>hi</sup> (pink line), and correlated with overall survival. Solid black line indicates 50% median survival. *P*-value was calculated using log-rank statistical test.
- Kaplan–Meier survival graph depicts 74 metastasis-free melanoma patients from the TCGA database divided into four groups according to tumor (T) stage at diagnosis combined with C-MYC protein expression levels (low/T(0-2), solid blue line; high/T(0-2), solid pink line; low/T(4b), stippled blue line; high/T(4b), stippled pink line). Solid line black indicates 50% median survival. *P*-values were calculated using log-rank statistical test.
- Kaplan–Meier survival graph plots AMPK $\alpha$  protein expression levels of 127 melanoma patients derived from TCGA database, divided into two groups AMPK $\alpha$ <sup>lo</sup> (blue line) versus AMPK $\alpha$ <sup>hi</sup> (pink line), and correlated with overall survival. Solid black line indicates 50% median survival. *P*-value was calculated using log-rank statistical test.

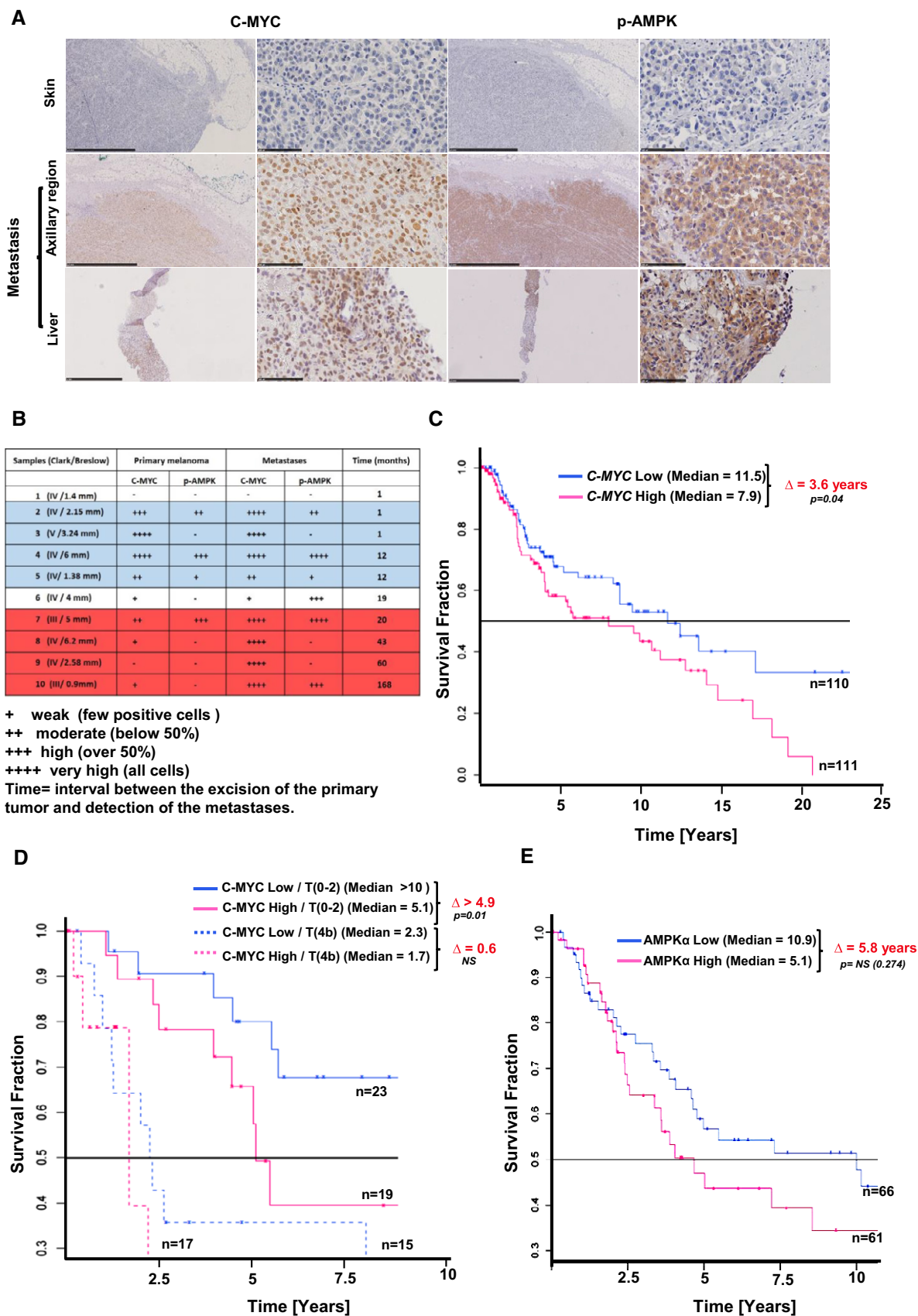


Figure 9.

that there is no functional redundancy with the other Myc family members.

Our studies using *c-Myc<sup>rep</sup>* mice to monitor c-Myc protein expression during melanoma progression show that only a minor fraction of melanoma cells are c-Myc positive at the primary tumor site. Nonetheless, protein expression levels and frequency of c-Myc-positive cells are increased at metastatic sites. A similar trend was observed in analysis of patient-derived cell lines or tumor samples with low or no C-MYC expression in melanoma from the primary tumor site and high expression at the site of metastasis. These findings are in agreement with previous reports showing that elevated C-MYC expression is preferentially observed in metastatic human melanoma patient samples correlating with and caused by copy number gains in *C-MYC* at 8q24 (Kraehn *et al*, 2001; Gerami *et al*, 2011; Pouryazdanparast *et al*, 2012a,b).

Moreover, melanoma patients with copy number gains at 8q24 often reveal aggressive clinical progression (Pouryazdanparast *et al*, 2012b). Our TCGA analysis of C-MYC expression in melanoma patients is in line with these reports and further extends our current knowledge. C-MYC protein expression, in particular at early tumor stage (T0-2), seems to be a significant predictor of reduced MST. Thus, assessing early lesions of melanoma patients for C-MYC expression would be important and could bear prognostic value.

We do not know whether elevated c-Myc expression at metastatic sites in our mouse melanoma model is also caused by gene amplification. Nevertheless, our transplantation experiments of c-Myc<sup>hi</sup> versus c-Myc<sup>lo</sup> melanoma cells demonstrated that c-Myc-positive melanoma cells are more aggressive and have a higher tumor initiation potential compared to c-Myc-negative melanoma cells. Whether melanoma is hierarchically organized in phenotypically distinct subpopulations of tumorigenic versus non-tumorigenic is controversially discussed (Quintana *et al*, 2008, 2010; Schatton *et al*, 2008; Boiko *et al*, 2010; Civenni *et al*, 2011).

c-Myc expression in murine melanoma causes a constitutive growth program upregulating associated gene expression signatures including RNA biosynthesis, RNA processing, transcription, and metabolism being in agreement with the role of Myc reported in other cancers (Eilers & Eisenman, 2008; Dang *et al*, 2009). All cellular processes, including metabolism, have to adapt to manage increased energy consumption and production of macromolecules in order to cope with proliferative stress to ensure survival of tumor cells. In this context, we focused on AMPK, as it is a central energy and redox sensor. AMPK is activated by metabolic stresses, which lower the cellular energy status by decreasing catabolic generation of ATP or accelerating ATP consumption. Upon activation, it functions to restore cellular energy homeostasis by switching off anabolic pathways and other ATP-consuming processes while switching on ATP-producing catabolic pathways (Hardie *et al*, 2012). The role of AMPK in cancer is complex and context dependent. Historically, AMPK was first associated with tumor suppressive functions based on the discovery that the tumor suppressor serine-threonine kinase liver kinase B1 is a direct activator of AMPK (Woods *et al*, 2003; Shaw *et al*, 2004). The ability of AMPK to activate the tuberous sclerosis complex, a negative regulator of mTORC1 and frequently

activated in cancer through upstream activators such as PI3K and AKT, further suggested that AMPK plays a tumor suppressive role (Lizcano *et al*, 2004; Inoki *et al*, 2006). Genetic loss of studies showing that inactivation of AMPK accelerates tumor growth in an experimental model of lymphomagenesis is also in agreement with a tumor suppressive function of AMPK (Faubert *et al*, 2013). Although AMPK has been associated with tumor suppressive functions, there is accumulating evidence that activation of AMPK can act pro-tumorigenic in a context-dependent manner (Hardie, 2015). AMPK has been shown to be important in oncogene-induced tumorigenesis as in Hras<sup>V12</sup> ± PTEN-induced astrocytic tumor cell proliferation (Rios *et al*, 2013) and kinase suppressor of Ras 2-induced anoikis resistance of MEFs and several cancer cell lines (Fernandez *et al*, 2012). Interestingly, AMPK-related kinase 5 (ARK5) was identified in a synthetic lethal RNAi screen for kinases that are selectively required to support tumor cells when Myc is overexpressed (Liu *et al*, 2012). Depletion of ARK5 prolonged survival in Myc-driven hepatocellular carcinoma mouse models. Inhibition of AMPK signaling in Myc-expressing cells resulted in cellular ATP collapse and caused increased levels of reactive oxygen species causing apoptosis (Liu *et al*, 2012). A similar role has been suggested for AMPK regulating NADPH homeostasis to promote tumor cell survival under circumstances of energy stress (Jeon *et al*, 2012). In a murine myeloid leukemia model, AMPK protected leukemia-initiating cells from metabolic stress via suppression of ROS (Saito *et al*, 2015). Our results are in line with these reports showing that survival of c-Myc<sup>hi</sup> Nras<sup>Q61K</sup>-driven *INK4a*-mutant melanoma cells activates and is dependent on AMPK signaling to maintain ATP homeostasis and to suppress oxidative stress. Interestingly, specific AMPK subunits/isoforms (AMPK $\alpha$ 1 and AMPK $\beta$ 2) are amplified in various human tumors and coincide with activation and/or amplifications of various oncogenes including KRAS, BRAF, AKT, and C-MYC across several cancer types such as breast, bladder cancer, and melanoma (Monteverde *et al*, 2015). These reports combined with our results support a pro-tumorigenic role of AMPK signaling. Therefore, it is likely that its role is multifaceted and context dependent.

In conclusion, our results reveal an important AMPK-dependent oncogenic mechanism by which c-Myc-positive melanomas ensure survival coping with tumor gene-induced proliferative stress including suppression of oxidative stress. Moreover, we show that C-MYC protein expression at an early stage of human melanoma has prognostic value for melanoma patients.

## Materials and Methods

### Mice

*Tyr::Nras<sup>Q61K</sup>INK4a<sup>-/-</sup>* mice were previously described (Ackermann *et al*, 2005) and crossed to *c-Myc<sup>lox/lox</sup>* (Trumpp *et al*, 2001) and *c-Myc<sup>G/G</sup>* (Huang *et al*, 2008) to generate *Tyr::Nras<sup>Q61K</sup>INK4a<sup>-/-</sup>c-Myc<sup>lox/lox</sup>* and *c-Myc<sup>G/G</sup>Tyr::Nras<sup>Q61K</sup>INK4a<sup>-/-</sup>* (*c-Myc<sup>rep</sup>*), respectively. *Tyr::Nras<sup>Q61K</sup>INK4a<sup>-/-</sup>c-Myc<sup>lox/lox</sup>* were crossed to a melanocyte-specific Cre line—*Tyr::Cre* (Delmas *et al*, 2003) to generate *Tyr::Nras<sup>Q61K</sup>INK4a<sup>-/-</sup>c-Myc<sup>Δ/Δ</sup>*. *Rag2<sup>γc<sup>-/-</sup></sup>* (B6.Rag2<sup>tm1Fwa</sup>Il2g<sup>tmWjl</sup>) and NSG (NOD.Cg-Prkdc<sup>scid</sup> Il2r<sup>tm1Wjl</sup>/

SzJ) were purchased from TACONIC and the Jackson Laboratories (United States).

### Cell lines

Human melanoma cell lines have been described (Caballero *et al*, 2010; Nikolaev *et al*, 2011) and were cultured in RPMI1640 media supplemented with 10% FCS and 50 µg/ml gentamycin (RPMI10). Primary mouse melanoma cell lines (mM1, mM2, mM3) were cultured in RPMI10 supplemented with 5 µg/ml insulin (Sigma), 100 ng/ml  $\alpha$ -MSH (Sigma), 25 ng/ml FGF (Invitrogen), 200 ng/ml TPA (Sigma), 30 ng/ml endothelin3 (Sigma), and 5 µM dexamethasone (AppliChem). GFP-IRES-Cre-ERT stable cell lines (mM1 and mM2) were generated transducing a GFP-IRES-Cre-ERT construct. GFP<sup>+</sup> cells were FACS sorted and expanded.

### Single cell preparation of primary, metastatic, and s.c. melanomas

Tumors were minced into small pieces and digested using dispase (4 mg/ml, Gibco) and collagenase (1 mg/ml, Gibco) for 2 h at 37°C. Cell clumps were removed using a quick spin. Supernatant containing the single cell suspension was collected and filtered (40 µm cell strainer). Washing steps were repeated 3×. Two additional washes with 1× HBSS (without Mg<sup>2+</sup> and Ca<sup>2+</sup>) were performed prior to FACS staining or s.c. injections.

### Immunohistochemistry

Mouse organs and primary patient samples (obtained from the Department of Pathology of CHUV, Lausanne) were fixed with 4% paraformaldehyde (4°C) and embedded in paraffin; 3-µm sections were stained with H&E using standard methods. Anti-c-Myc (Y69, Abcam) staining was performed according to manufacturer's instructions.

### Flow cytometry

Single cell suspensions of *c-Myc<sup>crep</sup>* mice ( $5 \times 10^5$ – $1 \times 10^6$  cells) were resuspended in staining media (SM; 1× HBSS, 2% FCS), stained with  $\alpha$ -CD31 and  $\alpha$ -CD45 using standard flow cytometric staining procedures, and analyzed on a Dako CyAn Flow Cytometer for GFP expression; dead cells were excluded using DAPI (CD31<sup>-</sup>CD45<sup>-</sup>DAPI<sup>-</sup>). Data were processed using FlowJo<sup>®</sup> software. For subsequent RNA-seq and s.c. transplantation assays, cells were sorted using a BC MoFlo Astrios<sup>EQ</sup> cell sorter. Purity of GFP<sup>+</sup> and GFP<sup>-</sup> live cell populations (CD31<sup>-</sup>CD45<sup>-</sup>DAPI<sup>-</sup>) was >90%.

### s.c. transplantation *in vivo*

*In vivo* transplantation assays were performed using sorted primary cell populations from *c-Myc<sup>crep</sup>* mice (1,000 cells per recipient NSG mouse of either GFP<sup>lo</sup> or GFP<sup>hi</sup> (CD31<sup>-</sup>CD45<sup>-</sup>DAPI<sup>-</sup>) fraction) or using the mM1 or mM3 cell lines transplanting  $1 \times 10^5$  cells s.c. into Rag2 $\gamma_c^{-/-}$  mice. Cells were injected into the flank of recipient mice in 100 µl of Matrigel<sup>™</sup>. Once tumor volumes reached 50–100 mm<sup>3</sup> in the cell line transplantation assays, c-Myc

expression was inhibited using (–), (+)JQ1 at 50 mg/kg/day injecting mice i.p.

### RNA-seq

Total RNA was prepared from GFP<sup>hi</sup> or GFP<sup>lo</sup> FACS-sorted cells and collected in triplicates using RNAqueous-Micro kit (Ambion). RNA-seq was performed by the Genomic Technologies Facility platform (University of Lausanne, Switzerland). An RNA amplification step was done using Ovation<sup>®</sup> RNA Amplification System V2 (Nugen). The Ovation<sup>®</sup> Ultralow Library System V2 (Nugen) was used for library preparation. Library sequencing was done using an Illumina HiSeq 2500 sequencer. RNA-seq mapping and analysis are described in the Appendix Supplementary Methods.

### Antibodies and Western blotting

Western analysis was performed under standard methods. All antibodies used in this study are listed in the Appendix Table S1.

### Cell proliferation and apoptosis detection

Cell proliferation was analyzed using the alamarBlue<sup>®</sup> cell viability reagent (Invitrogen) according to manufacturer's instructions. Melanoma cells were plated (2,500 cells/well). Cells were treated 24 h post-seeding with different compounds and harvested at different time points as indicated. Each condition was done in triplicates. Total apoptotic cells were assessed by AnnexinV-Cy5/7AAD staining using the AnnexinV-Cy5 Apoptosis Detection Kit (BD Biosciences) according to manufacturer's instructions. Samples were analyzed on a Dako CyAn Flow Cytometer and data processed using FlowJo<sup>®</sup> software.

### siRNA

siRNA transfections were performed using Lipofectamine RNAiMAX (Invitrogen) according to manufacturer's manual. Different siRNAs were purchased as smartPools (FlexiTube GeneSolution, GS17869) from Qiagen. Allstar negative control (Qiagen, SI03650318) was used as negative control.

### *In vitro* assays

#### ROS staining

ROS analysis was detected using H2DCFDA (Sigma) staining. Twenty-five thousand cells were stained with H2DCFDA at a final concentration of 50 µM. Cells were incubated for 45–60 min under standard culture conditions (37°C, 5% CO<sub>2</sub>), and then, H2DCFDA fluorescence was analyzed on a Dako CyAn Flow Cytometer. Data were processed using FlowJo<sup>®</sup> software. Each condition was analyzed in triplicates in three independent experiments.

#### c-Myc inhibition

c-Myc depletion in *c-Myc<sup>lox/lox</sup>Cre-ERT*-expressing cells was induced treating cells with 4-hydroxy-tamoxifen (4-OHT) (Sigma) at a final concentration of 1 µM in ethanol (ETOH). ETOH was used as vehicle control. c-Myc expression was downregulated treating



cells with the BRD4 inhibitor (+)JQ1 (Selleckchem) at a final concentration of 1  $\mu$ M. The (–)JQ1 (Sigma, 1  $\mu$ M) inactive enantiomer was used as control.

#### AMPK pathway modulation

AMP-activated protein kinase pathway signaling was inhibited treating the cells with dorsomorphin (Sigma, 10  $\mu$ M). AMPK pathway activation was induced treating cells with 991 (5-([6-chloro-5-(1-methylindol-5-yl)-1H-benzimidazol-2-yl]oxy)-2-methyl-benzoic acid (Bultot et al, 2016); compound at a final concentration of 10  $\mu$ M.

#### Antioxidant treatment

$\alpha$ -tocopherol (Sigma; 100  $\mu$ M) was used as antioxidant treatment to counteract ROS-induced apoptosis. Cells were pretreated with  $\alpha$ -tocopherol for 24 h and subsequently maintained continuously in the media for the whole experiment.

#### Kaplan–Meier and statistical analysis

Protein and RNA-seq expression levels from melanoma patients were downloaded from the TCGA website. Kaplan–Meier survival curves were created with *survfit* function from the survival R package and statistical comparisons with the function *comp* from the survMisc R package. For comparison of pooled data between two groups, unpaired *t*-tests were used to determine significance (\* $P < 0.05$ , \*\* $P < 0.03$ , \*\*\* $P < 0.01$ ).

#### Adenine nucleotide measurements

Sample preparation for adenine nucleotide analysis was based on Gheldof et al (2017), see Appendix Supplementary Methods.

#### Ethics statement

All animal work was conducted according to Swiss national guidelines. All mice were kept in the animal facility under EPFL animal care regulations. This study has been reviewed and approved by the cantonal veterinary office.

**Expanded View** for this article is available online.

#### Acknowledgements

This work was in part supported by the Swiss National Science Foundation and the Swiss Cancer League to F.R. We would like to acknowledge Christelle Dubey, Laure Bardouillet, Pasqualina Magliano, and Marianne Nkosi for technical assistance, Lionel Larue for providing the Tyr::Cre. We would like to thank Aleksandra Radenovic, Jose Artacho, the histology team, and Sintia Winkler for technical assistance with microscopy, histology, and flow cytometry. We would like to thank Gisele Ferrand for guidance and advice concerning animal experiments as well as the DNA array facility of the University of Lausanne for RNA sequencing and technical analysis.

#### Author contributions

AK, MA, CC, JS-D, MPG, and SC performed experiments and analyzed data. ML performed statistical and data base analysis. LL analyzed pathological slides from human melanoma patients. UK, AT, SM, KS, and FB analyzed data and provided conceptual and experimental guidance throughout the study and

helped writing the manuscript. FR conceived the study, analyzed data, and wrote the manuscript.

#### Conflict of interest

C. Collodet, M.P. Giner, S. Christen, S. Moco, and K. Sakamoto are employees of the Nestlé Institute of Health Sciences SA (Switzerland). The remaining authors declare that they have no conflict of interest.

## References

- Ackermann J, Fruttschi M, Kaloulis K, McKee T, Trumpp A, Beermann F (2005) Metastasizing melanoma formation caused by expression of activated N-RasQ61K on an INK4a-deficient background. *Can Res* 65: 4005–4011
- Berger MF, Hodis E, Heffernan TP, Deribe YL, Lawrence MS, Protopopov A, Ivanova E, Watson IR, Nickerson E, Ghosh P, Zhang H, Zeid R, Ren X, Cibulskis K, Sivachenko AY, Wagle N, Sucker A, Sougnez C, Onofrio R, Ambrogio L et al (2012) Melanoma genome sequencing reveals frequent PREX2 mutations. *Nature* 485: 502–506
- Beroukhir M, Mermel CH, Porter D, Wei G, Raychaudhuri S, Donovan J, Barretina J, Boehm JS, Dobson J, Urashima M, Mc Henry KT, Pinchback RM, Ligon AH, Cho YJ, Haery L, Greulich H, Reich M, Winckler W, Lawrence MS, Weir BA et al (2010) The landscape of somatic copy-number alteration across human cancers. *Nature* 463: 899–905
- Boiko AD, Razorenova OV, van de Rijn M, Swetter SM, Johnson DL, Ly DP, Butler PD, Yang GP, Joshua B, Kaplan MJ, Longaker MT, Weissman IL (2010) Human melanoma-initiating cells express neural crest nerve growth factor receptor CD271. *Nature* 466: 133–137
- Bultot L, Jensen TE, Lai YC, Madsen AL, Collodet C, Kviklyte S, Deak M, Yavari A, Foretz M, Ghaffari S, Bellahcene M, Ashrafian H, Rider MH, Richter EA, Sakamoto K (2016) Benzimidazole derivative small-molecule 991 enhances AMPK activity and glucose uptake induced by AICAR or contraction in skeletal muscle. *Am J Physiol Endocrinol Metab* 311: E706–E719
- Caballero OL, Zhao Q, Rimoldi D, Stevenson BJ, Svobodova S, Devalle S, Rohrig UF, Pagotto A, Michielin O, Speiser D, Wolchok JD, Liu C, Pejovic T, Odunsi K, Brasseur F, Van den Eynde BJ, Old LJ, Lu X, Cebon J, Strausberg RL et al (2010) Frequent MAGE mutations in human melanoma. *PLoS One* 5: e12773
- Chin L (2003) The genetics of malignant melanoma: lessons from mouse and man. *Nat Rev Cancer* 3: 559–570
- Chin L, Garraway LA, Fisher DE (2006) Malignant melanoma: genetics and therapeutics in the genomic era. *Genes Dev* 20: 2149–2182
- Civenni G, Walter A, Kobert N, Mihic-Probst D, Zipser M, Belloni B, Seifert B, Moch H, Dummer R, van den Broek M, Sommer L (2011) Human CD271-positive melanoma stem cells associated with metastasis establish tumor heterogeneity and long-term growth. *Can Res* 71: 3098–3109
- Crute BE, Seefeld K, Gamble J, Kemp BE, Witters LA (1998) Functional domains of the alpha1 catalytic subunit of the AMP-activated protein kinase. *J Biol Chem* 273: 35347–35354
- Curtin JA, Fridlyand J, Kageshita T, Patel HN, Busam KJ, Kutzner H, Cho KH, Aiba S, Brocker EB, LeBoit PE, Pinkel D, Bastian BC (2005) Distinct sets of genetic alterations in melanoma. *N Engl J Med* 353: 2135–2147
- Dang CV, Le A, Gao P (2009) MYC-induced cancer cell energy metabolism and therapeutic opportunities. *Clin Cancer Res* 15: 6479–6483
- Dejure FR, Eilers M (2017) MYC and tumor metabolism: chicken and egg. *EMBO J* 36: 3409–3420
- Delmas V, Martinuzzi S, Bourgeois Y, Holzenberger M, Larue L (2003) Cre-mediated recombination in the skin melanocyte lineage. *Genesis* 36: 73–80



- Delmore JE, Issa GC, Lemieux ME, Rahl PB, Shi J, Jacobs HM, Kastritis E, Gilpatrick T, Paranal RM, Qi J, Chesi M, Schinzel AC, McKeown MR, Heffernan TP, Vakoc CR, Bergsagel PL, Ghobrial IM, Richardson PG, Young RA, Hahn WC *et al* (2011) BET bromodomain inhibition as a therapeutic strategy to target c-Myc. *Cell* 146: 904–917
- Eilers M, Eisenman RN (2008) Myc's broad reach. *Genes Dev* 22: 2755–2766
- Faubert B, Boily G, Izreig S, Griss T, Samborska B, Dong Z, Dupuy F, Chambers C, Fuerth BJ, Viollet B, Mamer OA, Avizonis D, DeBerardinis RJ, Siegel PM, Jones RG (2013) AMPK is a negative regulator of the Warburg effect and suppresses tumor growth *in vivo*. *Cell Metab* 17: 113–124
- Fernandez MR, Henry MD, Lewis RE (2012) Kinase suppressor of Ras 2 (KSR2) regulates tumor cell transformation via AMPK. *Mol Cell Biol* 32: 3718–3731
- Gerami P, Jewell SS, Pouryazdanparast P, Wayne JD, Haghight Z, Busam KJ, Rademaker A, Morrison L (2011) Copy number gains in 11q13 and 8q24 [corrected] are highly linked to prognosis in cutaneous malignant melanoma. *J Mol Diagn* 13: 352–358
- Gray-Schopfer V, Wellbrock C, Marais R (2007) Melanoma biology and new targeted therapy. *Nature* 445: 851–857
- Hardie DG, Ross FA, Hawley SA (2012) AMPK: a nutrient and energy sensor that maintains energy homeostasis. *Nat Rev Mol Cell Biol* 13: 251–262
- Hardie DG (2015) Molecular pathways: is AMPK a friend or a foe in cancer? *Clin Cancer Res* 21: 3836–3840
- Huang CY, Bredemeyer AL, Walker LM, Bassing CH, Sleckman BP (2008) Dynamic regulation of c-Myc proto-oncogene expression during lymphocyte development revealed by a GFP-c-Myc knock-in mouse. *Eur J Immunol* 38: 342–349
- Inoki K, Ouyang H, Zhu T, Lindvall C, Wang Y, Zhang X, Yang Q, Bennett C, Harada Y, Stankunas K, Wang CY, He X, MacDougald OA, You M, Williams BO, Guan KL (2006) TSC2 integrates Wnt and energy signals via a coordinated phosphorylation by AMPK and GSK3 to regulate cell growth. *Cell* 126: 955–968
- Jeon SM, Chandel NS, Hay N (2012) AMPK regulates NADPH homeostasis to promote tumour cell survival during energy stress. *Nature* 485: 661–665
- Kalkat M, De Melo J, Hickman KA, Lourenco C, Redel C, Resetka D, Tamachi A, Tu WB, Penn LZ (2017) MYC deregulation in primary human cancers. *Genes* 8: E151
- Kraehn GM, Utikal J, Udart M, Greulich KM, Bezold G, Kaskel P, Leiter U, Peter RU (2001) Extra c-myc oncogene copies in high risk cutaneous malignant melanoma and melanoma metastases. *Br J Cancer* 84: 72–79
- Kress TR, Sabo A, Amati B (2015) MYC: connecting selective transcriptional control to global RNA production. *Nat Rev Cancer* 15: 593–607
- Laurenti E, Wilson A, Trumpp A (2009) Myc's other life: stem cells and beyond. *Curr Opin Cell Biol* 21: 844–854
- Liu L, Ulbrich J, Muller J, Wustefeld T, Aeberhard L, Kress TR, Muthalagu N, Rycak L, Rudalska R, Moll R, Kempa S, Zender L, Eilers M, Murphy DJ (2012) Deregulated MYC expression induces dependence upon AMPK-related kinase 5. *Nature* 483: 608–612
- Lizcano JM, Goransson O, Toth R, Deak M, Morrice NA, Boudeau J, Hawley SA, Udd L, Makela TP, Hardie DG, Alessi DR (2004) LKB1 is a master kinase that activates 13 kinases of the AMPK subfamily, including MARK/PAR-1. *EMBO J* 23: 833–843
- Loven J, Hoke HA, Lin CY, Lau A, Orlando DA, Vakoc CR, Bradner JE, Lee TI, Young RA (2013) Selective inhibition of tumor oncogenes by disruption of super-enhancers. *Cell* 153: 320–334
- Maldonado JL, Fridlyand J, Patel H, Jain AN, Busam K, Kageshita T, Ono T, Albertson DG, Pinkel D, Bastian BC (2003) Determinants of BRAF mutations in primary melanomas. *J Natl Cancer Inst* 95: 1878–1890
- Mihaylova MM, Shaw RJ (2011) The AMPK signalling pathway coordinates cell growth, autophagy and metabolism. *Nat Cell Biol* 13: 1016–1023
- Monteverde T, Muthalagu N, Port J, Murphy DJ (2015) Evidence of cancer-promoting roles for AMPK and related kinases. *FEBS J* 282: 4658–4671
- Nesbit CE, Tersak JM, Prochownik EV (1999) MYC oncogenes and human neoplastic disease. *Oncogene* 18: 3004–3016
- Nikolaev SI, Rimoldi D, Iseli C, Valsesia A, Robyr D, Gehrig C, Harshman K, Guipponi M, Bukach O, Zoete V, Michielin O, Muehlethaler K, Speiser D, Beckmann JS, Xenarios I, Halazonetis TD, Jongeneel CV, Stevenson BJ, Antonarakis SE (2011) Exome sequencing identifies recurrent somatic MAP2K1 and MAP2K2 mutations in melanoma. *Nat Genet* 44: 133–139
- Pearce LR, Komander D, Alessi DR (2010) The nuts and bolts of AGC protein kinases. *Nat Rev Mol Cell Biol* 11: 9–22
- Pluskal T, Nakamura T, Villar-Briones A, Yanagida M (2010) Metabolic profiling of the fission yeast *S. pombe*: quantification of compounds under different temperatures and genetic perturbation. *Mol Biosyst* 6: 182–198
- Pouryazdanparast P, Brenner A, Haghight Z, Guitart J, Rademaker A, Gerami P (2012a) The role of 8q24 copy number gains and c-MYC expression in amelanotic cutaneous melanoma. *Mod Pathol* 25: 1221–1226
- Pouryazdanparast P, Cowen DP, Beilfuss BA, Haghight Z, Guitart J, Rademaker A, Gerami P (2012b) Distinctive clinical and histologic features in cutaneous melanoma with copy number gains in 8q24. *Am J Surg Pathol* 36: 253–264
- Pshenichnaya I, Schouwey K, Armario M, Larue L, Knoepfler PS, Eisenman RN, Trumpp A, Delmas V, Beermann F (2012) Constitutive gray hair in mice induced by melanocyte-specific deletion of c-Myc. *Pigment Cell Melanoma Res* 25: 312–325
- Purdue MP, Freeman LE, Anderson WF, Tucker MA (2008) Recent trends in incidence of cutaneous melanoma among US Caucasian young adults. *J Invest Dermatol* 128: 2905–2908
- Quintana E, Shackleton M, Sabel MS, Fullen DR, Johnson TM, Morrison SJ (2008) Efficient tumour formation by single human melanoma cells. *Nature* 456: 593–598
- Quintana E, Shackleton M, Foster HR, Fullen DR, Sabel MS, Johnson TM, Morrison SJ (2010) Phenotypic heterogeneity among tumorigenic melanoma cells from patients that is reversible and not hierarchically organized. *Cancer Cell* 18: 510–523
- Rios M, Foretz M, Viollet B, Prieto A, Fraga M, Costoya JA, Senaris R (2013) AMPK activation by oncogenesis is required to maintain cancer cell proliferation in astrocytic tumors. *Can Res* 73: 2628–2638
- Saito Y, Chapple RH, Lin A, Kitano A, Nakada D (2015) AMPK protects leukemia-initiating cells in myeloid leukemias from metabolic stress in the bone marrow. *Cell Stem Cell* 17: 585–596
- Schatton T, Murphy GF, Frank NY, Yamaura K, Waaga-Gasser AM, Gasser M, Zhan Q, Jordan S, Duncan LM, Weishaupt C, Fuhlbrigge RC, Kupper TS, Sayegh MH, Frank MH (2008) Identification of cells initiating human melanomas. *Nature* 451: 345–349
- Scortegagna M, Ruller C, Feng Y, Lazova R, Kluger H, Li JL, De SK, Rickert R, Pellicchia M, Bosenberg M, Ronai ZA (2014) Genetic inactivation or pharmacological inhibition of Pdk1 delays development and inhibits metastasis of Braf(V600E):Pten(–/–) melanoma. *Oncogene* 33: 4330–4339
- Shaw RJ, Kosmatka M, Bardeesy N, Hurler RL, Witters LA, DePinho RA, Cantley LC (2004) The tumor suppressor LKB1 kinase directly activates AMP-activated kinase and regulates apoptosis in response to energy stress. *Proc Natl Acad Sci USA* 101: 3329–3335
- Siegel R, Naishadham D, Jemal A (2013) Cancer statistics, 2013. *CA Cancer J Clin* 63: 11–30

- Trumpp A, Refaeli Y, Oskarsson T, Gasser S, Murphy M, Martin GR, Bishop JM (2001) c-Myc regulates mammalian body size by controlling cell number but not cell size. *Nature* 414: 768–773
- Vogt J, Traynor R, Sapkota GP (2011) The specificities of small molecule inhibitors of the TGF $\beta$ s and BMP pathways. *Cell Signal* 23: 1831–1842
- Woods A, Johnstone SR, Dickerson K, Leiper FC, Fryer LG, Neumann D, Schlattner U, Wallimann T, Carlson M, Carling D (2003) LKB1 is the upstream kinase in the AMP-activated protein kinase cascade. *Curr Biol* 13: 2004–2008
- Xia J, Jia P, Hutchinson KE, Dahlman KB, Johnson D, Sosman J, Pao W, Zhao Z (2014) A meta-analysis of somatic mutations from next generation sequencing of 241 melanomas: a road map for the study of genes with potential clinical relevance. *Mol Cancer Ther* 13: 1918–1928
- Xiao B, Sanders MJ, Carmena D, Bright NJ, Haire LF, Underwood E, Patel BR, Heath RB, Walker PA, Hallen S, Giordanetto F, Martin SR, Carling D, Gamblin SJ (2013) Structural basis of AMPK regulation by small molecule activators. *Nat Commun* 4: 3017
- Zhuang D, Mannava S, Grachtchouk V, Tang WH, Patil S, Wawrzyniak JA, Berman AE, Giordano TJ, Prochownik EV, Soengas MS, Nikiforov MA (2008) C-MYC overexpression is required for continuous suppression of oncogene-induced senescence in melanoma cells. *Oncogene* 27: 6623–6634